NACA

RESEARCH MEMORANDUM

THE HIGH-SPEED AERODYNAMIC EFFECTS OF MODIFICATIONS TO THE WING AND WING-FUSELAGE INTERSECTION OF AN AIRPLANE MODEL WITH THE WING SWEPT BACK 35°

By

Lee E. Boddy and Charles P. Morrill, Jr.

Ames Aeronautical Laboratory
Moffett Field, Calif.

NATIONAL ADVISORY COMMITTEE
FOR AERONAUTICS

WASHINGTON
February 18, 1948

NATIONAL ADVISORY COMMITTEE FOR AERONAUTICS

RESEARCH MEMORANDUM

THE HIGH-SPEED AERODYNAMIC EFFECTS OF MODIFICATIONS TO THE WING AND WING-FUSELAGE INTERSECTION OF AN AIRPLANE MODEL WITH THE WING SWEPT BACK 35°

By Lee E. Boddy and Charles P. Morrill, Jr.

SUMMARY

Wind-tunnel tests at high subsonic Mach numbers were conducted on a model of a pursuit airplane having a 35° swept-back wing. Tests were made to determine the effect of (1) the wing trailing-edge angle, (2) the fuselage contour at the wing-fuselage intersection, and (3) an extension at the leading edge of the wing root.

The results indicate that decreasing the wing trailing-edge angle eliminated (at least up to 0.90 Mach number) the reversal of pitching-moment and aileron hinge-moment characteristics noted at high Mach numbers for small angles of attack and aileron deflections with the true-contour wing. Contouring the fuselage side to the estimated shape of the undisturbed streamlines over the swept-back wing reduced the interference at the wing-fuselage intersection and improved the high-speed characteristics of the model. No benefits were derived from the wing leading-edge extension.

INTRODUCTION

Comparatively large angles of sweepback of wings and control surfaces are incorporated in the design of many current airplanes in order to delay the onset of compressibility effects. Since experimental data for highly swept lifting surfaces are rather incomplete, a series of wind-tunnel tests were conducted with a semispan model of a pursuit airplane having the wing swept back 35°.

During the tests several modifications were made to the wing and wing-fuselage intersection of the model, primarily to eliminate the reversal of pitching-moment and aileron hinge-moment characteristics noted for small angles of attack and aileron deflections at high Mach numbers, and to increase the divergence Mach number of the model to a value more closely approximating that predicted by simple theory. This report presents the results of that portion of the tests dealing with the modifications to the model. Subsequent reports will present the remainder of the data.

COEFFICIENTS AND SYMBOLS

The symbols used in this report are defined as follows:

V free-stream velocity, feet per second

q free-stream dynamic pressure $\left(\frac{1}{2}\rho V^2\right)$, pounds per square foot

M Mach number $\left(\frac{V}{\text{velocity of sound}}\right)$

S twice wing area of semispan model, square feet

M.A.C. wing mean aerodynamic chord, feet

b twice wing span of semispan model, feet

b_a aileron hinge-line length, feet

$\overline{c_a{}^2}$ mean-squared chord aft of aileron hinge line measured normal to the hinge line, square feet

C_L lift coefficient

$$\left(\frac{\text{twice lift of semispan model}}{qS}\right)$$

C_D drag coefficient

$$\left(\frac{\text{twice drag of semispan model}}{qS}\right)$$

C_m pitching-moment coefficient

$$\left(\frac{\text{twice pitching moment of semispan model}}{qS\ \text{M. A. C.}}\right)$$

C_{m_t} pitching-moment coefficient due to horizontal tail

C_{l_a} rolling-moment coefficient due to aileron

$$\left(\frac{\text{rolling moment due to aileron}}{qSb}\right)$$

C_{h_a} aileron hinge-moment coefficient

$$\left(\frac{\text{aileron hinge moment}}{qb_a\overline{c_a}^2}\right)$$

α angle of attack of fuselage reference line, degrees

δ_a aileron deflection about the hinge line, degrees

P pressure coefficient

$$\left[\frac{\text{(local static pressure)}-\text{(free-stream static pressure)}}{q}\right]$$

P_{cr} critical pressure coefficient (P at which the local velocity equals the local velocity of sound)

MODEL AND APPARATUS

All of the tests were conducted in the Ames 16-foot high-speed wind tunnel. To avoid the large interference and choking effects associated with strut-support systems at high Mach numbers, the reflection-plane method of mounting a semispan model was used. (See figs. 1 and 2.) A separation plate and fairing mounted on a turntable flush with the wind-tunnel wall served as the reflection plane and as a shield between the model and the tunnel boundary layer. Strips of metal fastened to the model maintained a 3/16-inch gap between the model and the separation plate. These strips were so attached that any leakage air would be directed in a vertical plane rather than horizontally across the wing or tail.

The model was of a low-wing pursuit airplane having the quarter-chord line of both the wing and the horizontal tail swept back approximately 35°. Tests were made with a true-contour wing and with an extended-chord wing (fig. 3), with a basic fuselage and with a modified fuselage contoured as shown in figure 4, and with a wing leading-edge extension as shown in figure 5.

Pertinent dimensions of the whole model (lateral dimensions twice those of semispan model) are as follows:

	True-contour wing	Extended-chord wing
Wing area, sq ft	10.980	11.516
Wing span, ft	7.423	7.423
Wing mean aerodynamic chord, ft	1.546	1.617
Wing root section (normal to quarter-chord line)	NACA 0012-64	NACA 0012-64 Modified
Wing tip section (normal to quarter-chord line)	NACA 0011-64	NACA 0011-64 Modified
Wing aspect ratio	5.02	4.785
Wing taper ratio	0.495	0.513
Sweepback of wing quarter-chord line, deg	35.2	35.4
Wing dihedral, deg	3.0	3.0
Incidence of wing root section, deg	1.00	1.00
Incidence of wing tip section, deg	– 1.00	– 1.00
Aileron hinge-line length, ft	2.008	2.008
Aileron mean-squared chord aft of hinge line (normal to hinge line), sq ft	0.1047	0.1545
Horizontal-tail area, sq ft	1.400	1.400
Sweepback of tail quarter-chord line, deg	34.59	34.59
Horizontal-tail dihedral, deg	10.0	10.0

RESULTS

Since no part of the support system was exposed to the main air stream, no corrections for tares have been applied to the data.

The effects of the wind-tunnel walls on the angle of attack, drag, and pitching moment have not been accounted for since they are small for a model of this size and in general have the opposite effect of the leakage. Also, no correction has been applied to the aileron effectiveness to account for the end-plate effect of the reflection plane. The aileron effectiveness of the half model agreed well with that obtained from preliminary tests of the whole model mounted in the center of the wind tunnel. However, constriction effects of the model and support system have been taken into account. As the model was small relative to the test section, the constriction correction to the Mach number was less than 2 percent at 0.90 Mach number.

Measurements of the boundary layer on the separation plate with the model removed indicated thicknesses of the order of one-fourth inch and one-half inch in the region of the wing and tail, respectively. Also, tuft studies with the model in place showed that the flow over the separation plate was smooth and steady at all Mach numbers and angles of attack used in the tests, although deviations of the flow direction in a vertical plane were noted near the gap between the model and the separation plate. The results shown in figure 6 are from pressure measurements taken with the model installed in order to determine the quality of the flow about the support system and model. It is evident that the gap between the tunnel wall and the separation plate was large enough to allow the tunnel boundary layer to pass through this space without spilling over the face of the separation plate. Furthermore, the gap was small enough to allow most of the fairing to be in the tunnel boundary layer, thus forestalling choking due to the fairing itself. Figure 6(b) indicates that no choking of the wind tunnel was encountered due either to the support system or the model.

The test Reynolds number varied from 3.35×10^6 at a Mach number of 0.30 to 6.20×10^6 at a Mach number of 0.90, based on a mean aerodynamic chord of 1.617 feet (fig. 7).

All moments are referred to a point 2.68 inches above the 25-percent point of the wing mean aerodynamic chord. This point corresponds to fuselage station 37.41 for the true-contour wing or station 37.70 for the extended-chord wing.

A summary of the lift and drag characteristics of the model with the true-contour wing is given in figure 8, and the aerodynamic characteristics of the model with the true-contour wing and with the extended-chord wing are compared in figures 9 to 14. The characteristics with the basic fuselage contour and with the modified contour are shown in figures 15 to 20, and the effect of the wing leading-edge extension is shown in figures 21 to 23. For the tests of the fuselage shapes, a band of pressure orifices was installed along the fuselage side approximately one-half inch from the upper surface of the wing.

Because of the relatively small size of the model, the data for low Mach numbers are inconsistent. Also, the drag coefficients shown are too large, due in part to the leakage air passing over the supporting structure inside the fairing. However, the variation with Mach number is believed to be reliable.

DISCUSSION

General Characteristics of the Original Model

The original model with the true-contour wing (NACA 0012-64 root section and NACA 0011-64 tip section measured normal to the quarter-chord line) had an average divergence Mach number of 0.87 for low lift coefficients. (See fig. 8.) Although no comparable data are available, this is 12 percent higher than is estimated for a similar unswept wing. Consideration of only the component of flow normal to the quarter-chord line would indicate a divergence Mach number 22 percent higher for a wing swept back 35° than for an unswept wing. It is indicated, then, that sweepback increased the divergence Mach number by a factor only slightly greater than half the secant of the sweepback angle.

At low Mach numbers the tail-off pitching-moment coefficient varied nonlinearly with lift coefficient in such a manner that the static longitudinal stability was less at the higher than at the lower lift coefficients. (See fig. 13.) As the Mach number was increased, the longitudinal stability decreased for low lift coefficients and increased for high lift coefficients. A general positive shift of the tail-off pitching moment was noted as the Mach number was increased.

Wing Trailing-Edge Contour

Measurements of the aileron hinge moments on the true-contour wing at the higher Mach numbers (fig. 9(a)) revealed a reversal of the variation of hinge moment with aileron deflection for small deflections. Since the ailerons had no nose balance, this undesirable reversal was attributed to the large trailing-edge angle, particularly when the same tendency, to a smaller degree, was noted in the pitching-moment characteristics of the wing. (See fig. 13.) Consequently the trailing edge of the model wing was extended 0.80 inch in a direction normal to the wing quarter-chord line and faired with flat sides to the points of tangency with the original contour, as shown in figure 3. This extension was approximately 4 percent of the root chord of the wing and 8 percent of the tip chord, and the trailing-edge angle measured normal to the quarter-chord line was reduced from 21.4° to 15.9° at the root and from 19.3° to 12.6° at the tip. The average trailing-edge angle of the aileron measured in a streamwise direction was reduced from 16.4° to 11.2°. As a result of this modification to the wing trailing edge, the overbalance of the aileron at high Mach numbers was completely eliminated (fig. 9(b)) and the tendency for the wing to become longitudinally unstable for low lift coefficients at 0.90 Mach number was overcome (fig. 13). Furthermore, the aileron effectiveness did not deteriorate as much at high Mach numbers, being two to three times as great at 0.90 Mach number for the modified wing as for the original wing. (See fig. 10.) The small improvement of aileron effectiveness at low speed is attributed to the comparatively larger size of the extended-chord aileron.

The lift and drag characteristics of the wing (figs. 11 and 12) were essentially unaffected by the trailing-edge extension except for an increase of lift-curve slope at the highest Mach number and possibly a small decrease of drag. The relatively large improvement of the drag characteristics at low speeds should be discounted because of the previously mentioned difficulty of measuring the forces at low speed with such a small model.

Figure 14(a) indicates no important changes of the tail characteristics due to the wing trailing-edge extension. A slight decrease of longitudinal stability due to the tail was noted where the wing lift-curve slope was increased, and the pitching-moment coefficient due to the tail was generally more negative with the modified wing. Consequently, the only major changes observed in the tail-on pitching-moment characteristics were the same as the improvements of the wing pitching-moment characteristics. (See fig. 14(b).)

No quantitative general conclusions concerning the trailing-edge contour can be made from the results previously discussed. It can be said only that, for the model considered here, reducing the trailing-edge angle eliminated the reversal of characteristics suffered by the true-contour wing. Perhaps a smaller modification would have been sufficient. It should be mentioned that the reversal is usually associated with changes of separation or boundary-layer growth near the trailing edge, or at supercritical Mach numbers with the chordwise movement of the shock waves. It follows, then, that airfoil section and angle of sweepback would be important factors in determining a suitable trailing-edge contour.

Wing-Fuselage Intersection

It has been pointed out that the increase of the divergence Mach number due to sweepback was not as great for this model as predicted by the simple cosine theory. Some deficiency may be expected, however, due in part to the restrictions on the air flow at the plane of symmetry. The streamlines in plan view tend to be S-shaped over a swept-back wing of finite thickness, but must be straight at the plane of symmetry, or conform to the shape of the fuselage at the wing-fuselage intersection. This restriction results in a spreading apart of the streamlines near the leading edge of the wing root and a crowding together of the streamlines near the trailing edge, as is indicated in figure 15 by the minimum-pressure peaks near 80 percent of the wing chord for the model with the basic fuselage.

The consequences of the restrictions on the air flow at the plane of symmetry of a swept-back wing are not clearly established. The general effect is an increase of the static pressure over the forward part of the wing root and a decrease of static pressure over the aft portion of the wing root. It follows then, that airfoil sections normally having their minimum-pressure point near or aft of the midchord would suffer additional reductions of minimum pressure near the plane of symmetry. Furthermore, the chordwise location of the minimum-pressure point probably would be forced rearward. Three detrimental effects would follow: (1) the local Mach number would be increased, (2) the tendency for separation of the air flow would be increased, and (3) in plan view the line of minimum pressure near the plane of symmetry would approach the normal to the streamlines thus enhancing the development of a shock front. It should be noted that these effects apply primarily to airfoil sections normally having their minimum-pressure point near or aft of the midchord. Negative pressure peaks near the leading edge would be reduced by the flow restrictions, and less detrimental effects would be expected.

An attempt was made to relieve this interference at the wing root by shaping the fuselage side to the estimated shape of the streamlines over the portion of a swept-back wing far distant from the root or tip. The streamline shape was estimated by assuming that only the component of the free-stream velocity normal to the wing quarter-chord line was affected by the pressure field of the wing, while the component parallel to the quarter-chord line remained unchanged. This assumption permitted calculation of the direction of the resultant velocity vector at each point along the chord of the wing. In order to avoid reduction of the fuselage cross-sectional area, the first modification consisted of enlarging the fuselage near the leading and trailing edges of the wing in such a manner that the direction of the streamlines along the wing-fuselage intersection corresponded to the calculated direction of the resultant velocity vector. Preliminary tests indicated no improvement of the high-speed characteristics of the model and revealed a serious minimum-pressure peak near the wing leading edge. Consequently, the fuselage contour was further modified so that the calculated lateral displacement of the streamlines due to the sweepback was about equally distributed on either side of the basic fuselage line. Hence the average pressure due to the modified fuselage should be approximately the same as that due to the basic fuselage. Also, the curvature of the forward part of the modification was reduced in order to eliminate the minimum-pressure peak obtained with the first modification. The final fuselage contour is compared with the basic contour in figure 4.

It should be noted that the vertical extent of the modification was limited by the depth of the fuselage, and that the flow over only the upper surface of the wing was affected due to the low position of the wing. Furthermore, the modified shape is probably not the optimum because it was designed to have approximately the same average effect on the static pressure over the wing as the basic fuselage. Both fuselages undoubtedly reduce the average pressure over the wing root.

In spite of the limitations, a more favorable pressure-recovery gradient and a smaller peak pressure was obtained at 0.90 Mach number with the modified wing-fuselage intersection (fig. 15). The high-speed lift and drag characteristics were considerably improved (figs. 16 and 17), the average divergence Mach number being increased approximately 0.02 (fig. 18). Although the modification was designed using the estimated pressure distribution over the wing upper surface for a lift coefficient near zero, the characteristics were improved for lift coefficients as high as 0.40.

Figures 19 and 20 indicate no important changes in the longitudinal stability characteristics of the wing due to the fuselage modification, but reveal a positive shift of the tail-off pitching moment at the higher Mach numbers and a slight decrease of the stability from the horizontal tail where the wing lift-curve slope was increased. Because of the improvement of the tail-off characteristics, the variation of the tail-on pitching-moment coefficient with Mach number was more satisfactory with the modified fuselage. An increase of Mach number always caused a climbing moment below a Mach number of 0.90 and a lift coefficient of 0.10. With the basic fuselage, a small diving moment was noted for all positive lift coefficients above a Mach number of 0.85.

In view of the appreciable gains made under the limited conditions of the tests, it is recommended that a more extensive investigation be carried out, including not only the effects of shaping the fuselage sides to the streamlines, but also the effects of other means of reducing the interference at the plane of symmetry. One method which should be studied is the modification of the airfoil section at the wing root, since this would be entirely independent of the fuselage position and would be applicable even to all-wing airplanes. Another method which might reduce the wing-fuselage interference is the judicious location and design of air inlets in the wing leading edge or the sides of the fuselage.

Wing Leading-Edge Extension

It has been shown that considerable disturbance of the air flow may occur at the plane of symmetry of a swept-back wing, so that the full advantage of sweepback is not realized. It seems probable, then, that modification of the critical center section so that its critical Mach number is higher relative to the outboard sections of the wing might improve the high-speed characteristics. The most straightforward way of doing this is to decrease the thickness-to-chord ratio at the root. For reasons of strength however, it is not practical to decrease the absolute thickness of the wing root. Consequently, the thickness-to-chord ratio of the root section was decreased by extending the leading edge forward at the root, as shown in figure 5. The extension was contoured so that the line of maximum thickness of the wing remained unchanged.

The results shown in figures 21 to 23 indicate no improvement of the lift, drag, or pitching-moment characteristics due to the leading-edge extension. Unfortunately, the extension interfered with many of the pressure orifices along the wing-fuselage intersection, so no satisfactory pressure data were obtained. However, there appeared to be a general reduction of the magnitude of the negative pressures over the wing root section. A more complete investigation is required to either overcome or explain the failure of the extension to improve the high-speed characteristics.

CONCLUSIONS

The results of the tests may be summarized as follows:

1. The wing with the true-contour sections exhibited serious reversal of pitching-moment and aileron hinge-moment characteristics for small angles of attack and aileron deflections at high Mach numbers. Extending the wing trailing edge to decrease the trailing-edge angle eliminated the reversals up to 0.90 Mach number.

2. The increase of divergence Mach number due to sweepback of the wings was only about half as great as predicted from simple theory. Since about one-fourth of the deficiency was overcome under limited conditions by contouring the fuselage side to the estimated shape of the undisturbed streamlines, further investigation should be directed toward the elimination of interference near the plane of symmetry of a swept-back wing.

3. Reduction of the thickness-to-chord ratio of the root section of the wing by extending the leading edge forward did not improve the high-speed characteristics.

Ames Aeronautical Laboratory,
National Advisory Committee for Aeronautics,
Moffett Field, Calif.

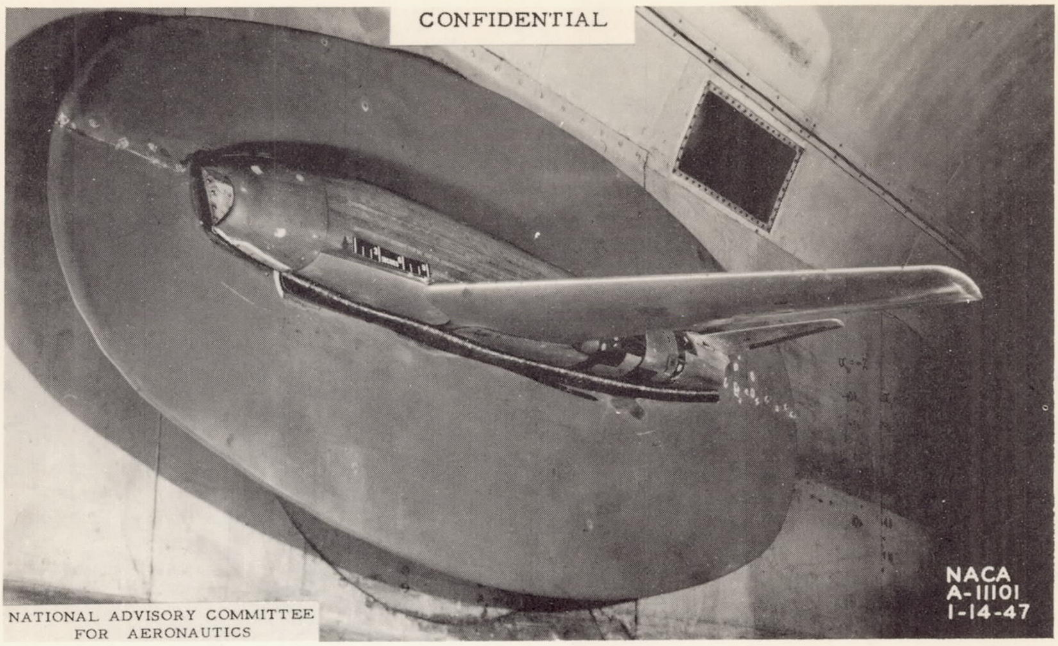

(a) Three-quarter front view.

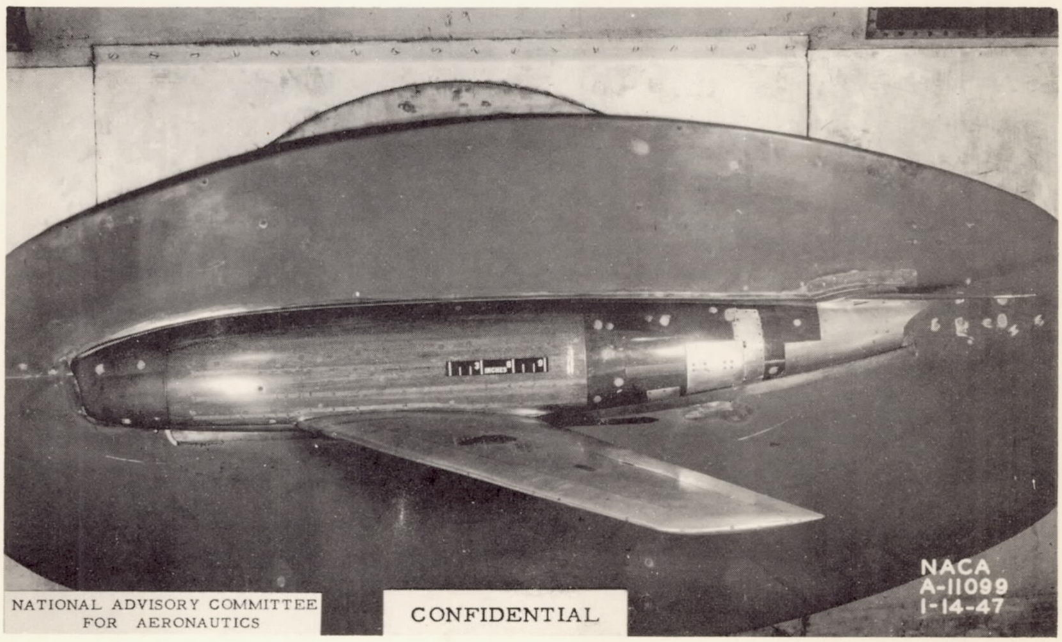

(b) Side view.

Figure 1.- Photographs of the model mounted in the wind tunnel.

CONFIDENTIAL

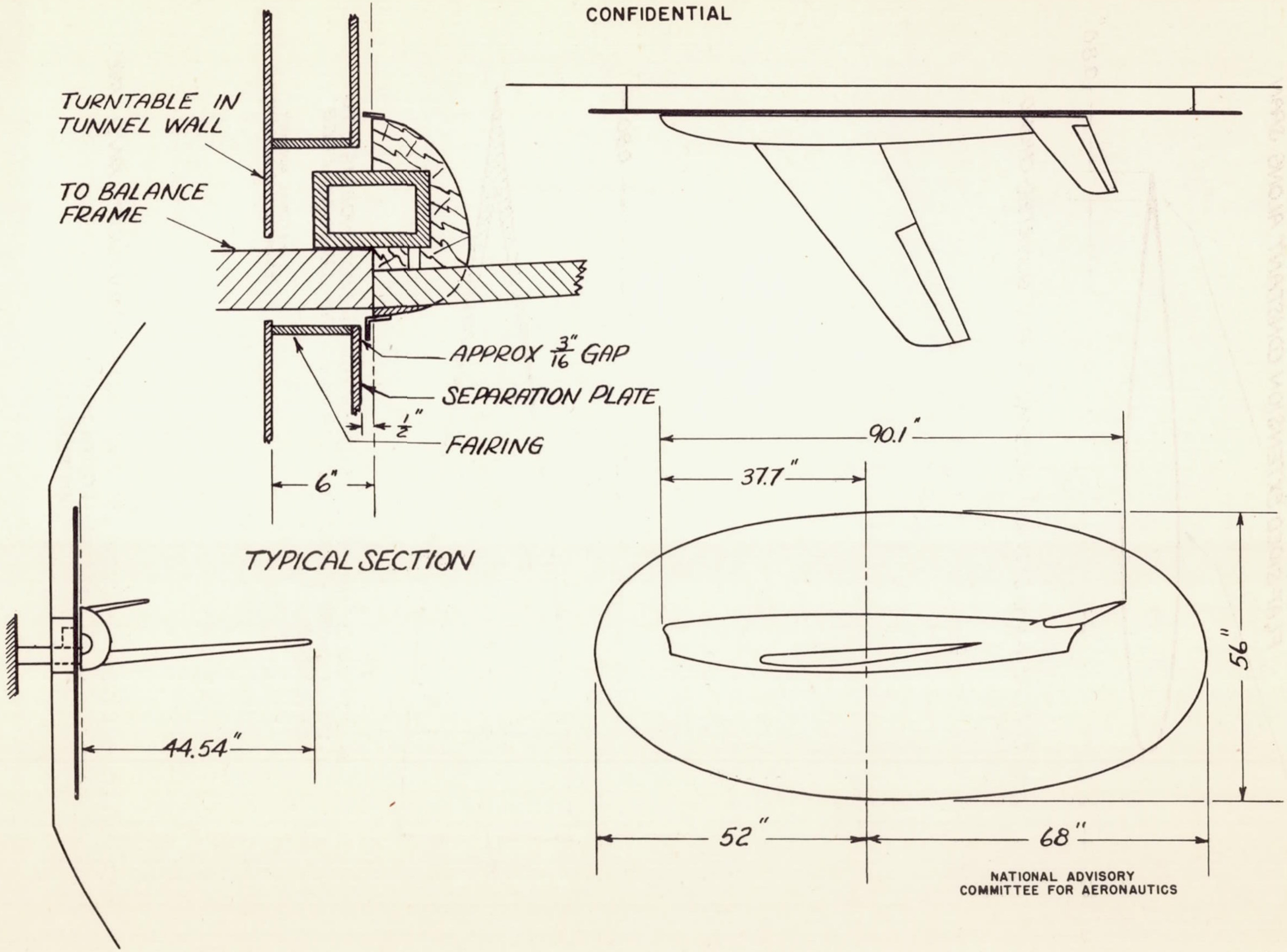

NATIONAL ADVISORY
COMMITTEE FOR AERONAUTICS

FIGURE 2. - SKETCHES OF THE MODEL INSTALLATION

CONFIDENTIAL

CONFIDENTIAL

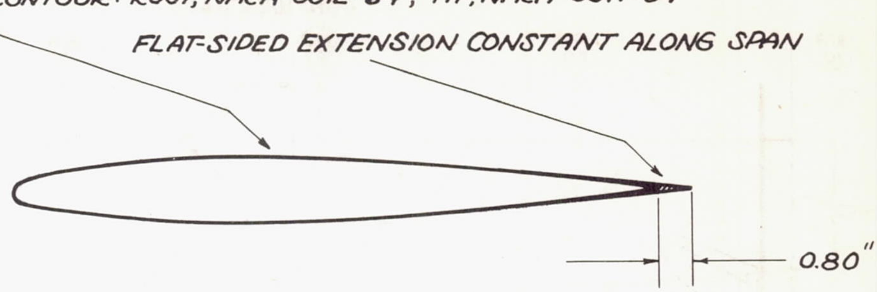

(a) TYPICAL WING SECTION NORMAL TO THE QUARTER-CHORD LINE.

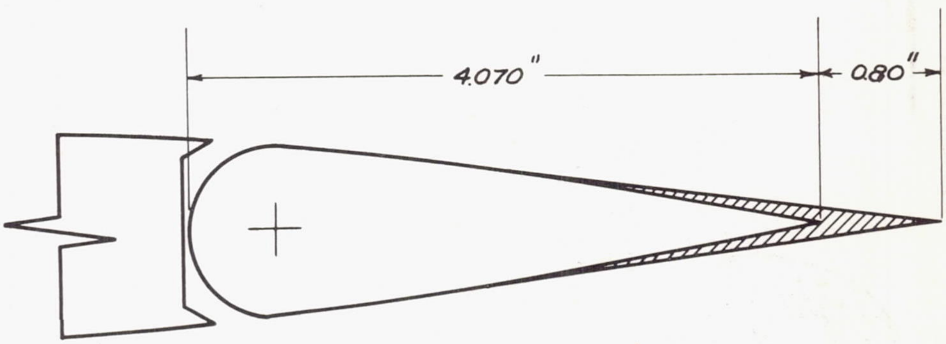

(b) SECTION OF THE WING THROUGH THE AILERON NORMAL TO THE QUARTER-CHORD LINE SHOWING THE TRAILING-EDGE EXTENSION.

NATIONAL ADVISORY
COMMITTEE FOR AERONAUTICS

FIGURE 3. - COMPARISON OF THE TRUE-CONTOUR AND THE EXTENDED-CHORD WING SECTIONS

CONFIDENTIAL

CONFIDENTIAL

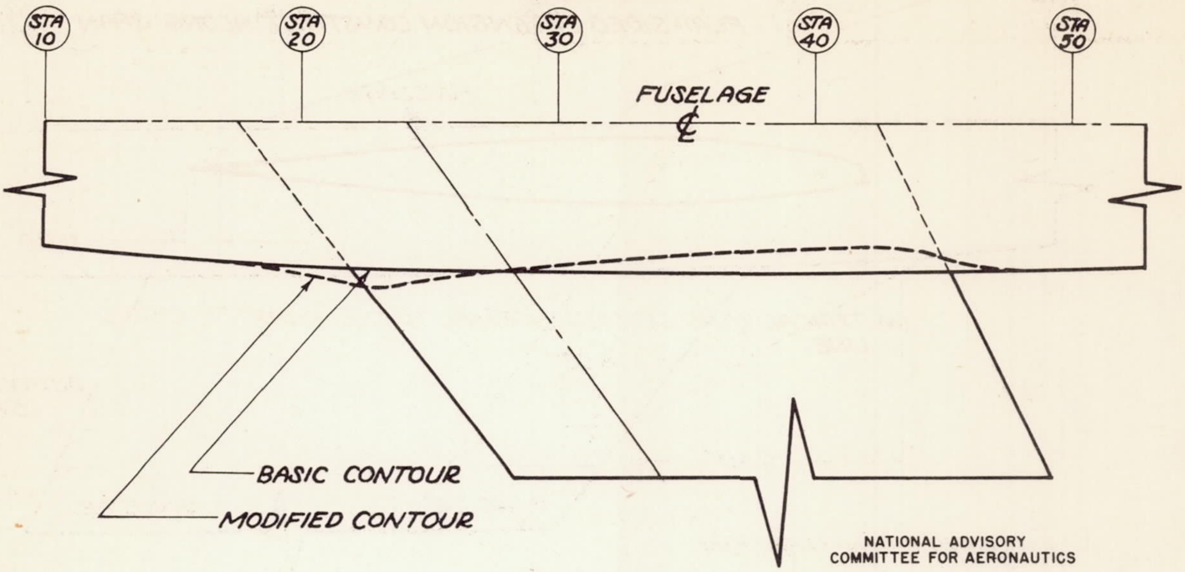

NATIONAL ADVISORY
COMMITTEE FOR AERONAUTICS

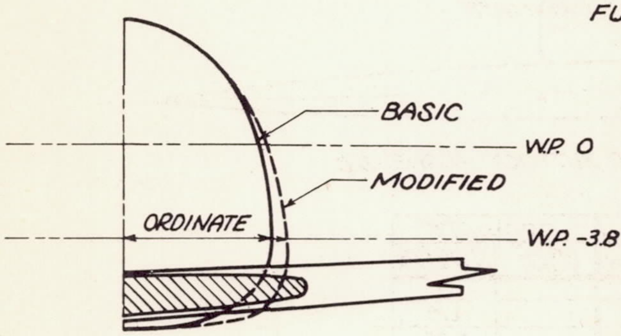

SECTION AT STATION 23

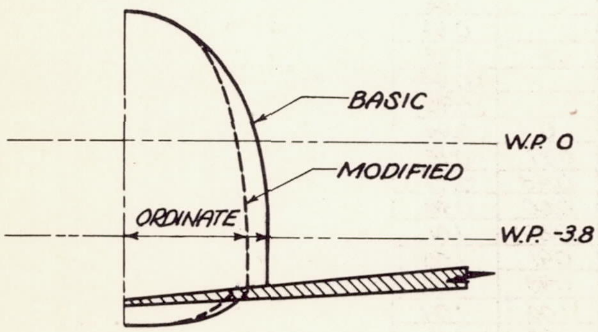

SECTION AT STATION 42

FUSELAGE ORDINATES AT WATER PLANE -3.8

FUSELAGE STATION	ORDINATES	
	BASIC CONTOUR	MODIFIED CONTOUR
16.0	5.55	5.55
18.0	5.65	5.74
20.0	5.80	5.99
21.0	5.84	6.17
22.0	5.87	6.43
22.5	5.88	6.51
23.0	5.90	6.48
23.5	5.93	6.44
24.0	5.93	6.38
25.0	5.95	6.26
26.0	5.95	6.14
28.0	6.00	5.95
30.0	6.01	5.77
32.0	6.01	5.57
34.0	6.01	5.41
36.0	5.98	5.27
38.0	5.95	5.15
40.0	5.90	5.06
42.0	5.85	5.00
44.0	5.79	5.05
45.0	5.77	5.29
45.5	5.75	5.38
46.0	5.73	5.46
46.5	5.71	5.51
47.0	5.68	5.54
48.0	5.62	5.56
50.0	5.51	5.50
52.0	5.38	5.39
54.0	5.27	5.27

FIGURE 4.- COMPARISON OF BASIC AND MODIFIED FUSELAGE CONTOURS

CONFIDENTIAL

CONFIDENTIAL

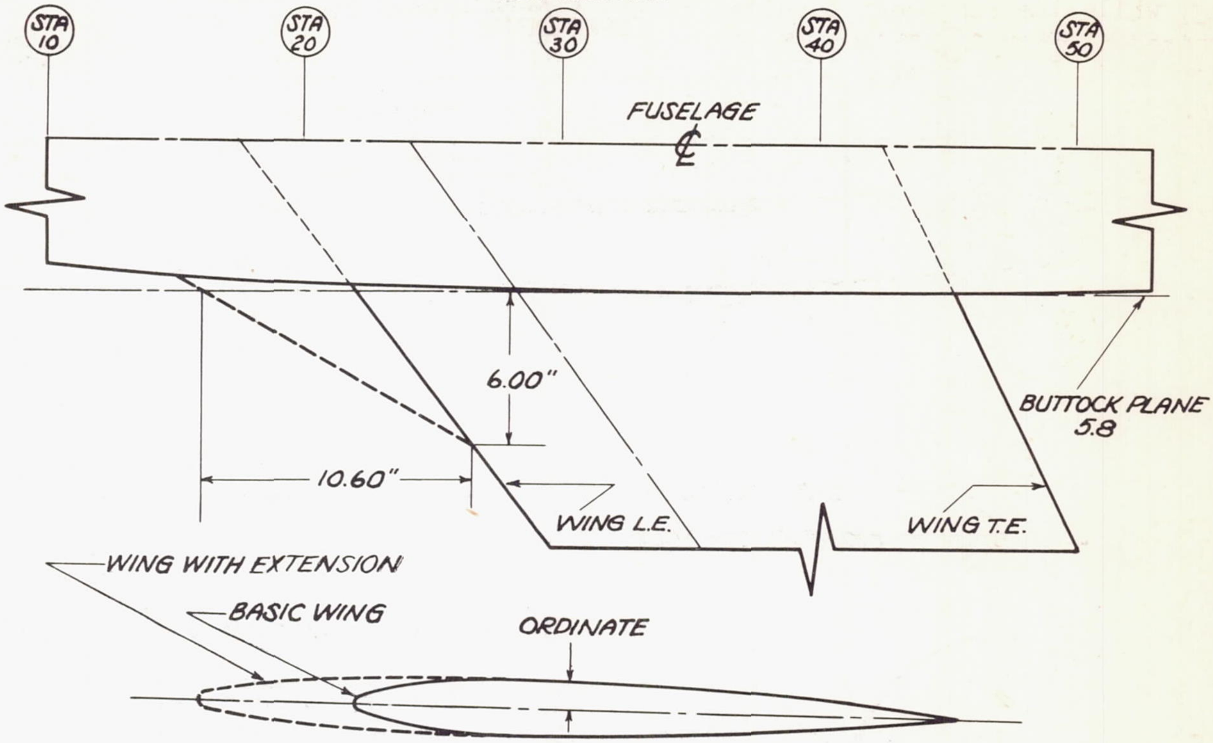

SECTION AT BUTTOCK PLANE 5.8

FUSELAGE STATION	ORDINATE	
	BASIC WING	WING AND EXTENSION
16.0		0
16.1		0.15
16.2		0.22
16.3		0.28
16.5		0.35
17.0		0.47
17.5		0.56
18.0		0.64
19.0		0.75
20.0		0.84
21.0		0.90
21.8	0	0.94
22.0	0.27	0.95
22.5	0.45	0.97
23.0	0.60	0.98
24.0	0.80	1.01
25.0	0.91	1.05
26.0	0.98	1.07
27.0	1.04	1.09
28.0	1.08	1.11
29.0	1.10	1.12
30.0	1.13	1.13

NATIONAL ADVISORY COMMITTEE FOR AERONAUTICS

FIGURE 5.- COMPARISON OF BASIC WING AND WING WITH LEADING-EDGE EXTENSION.

CONFIDENTIAL

CONFIDENTIAL

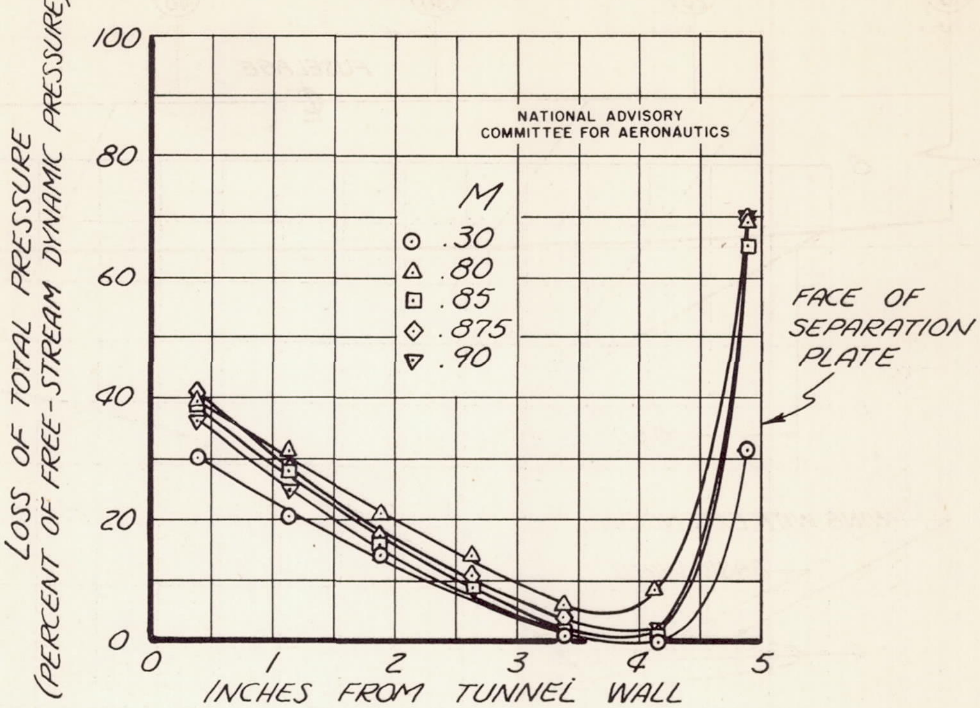

(a) LOSS OF TOTAL PRESSURE BETWEEN THE TUNNEL WALL AND THE SEPARATION PLATE

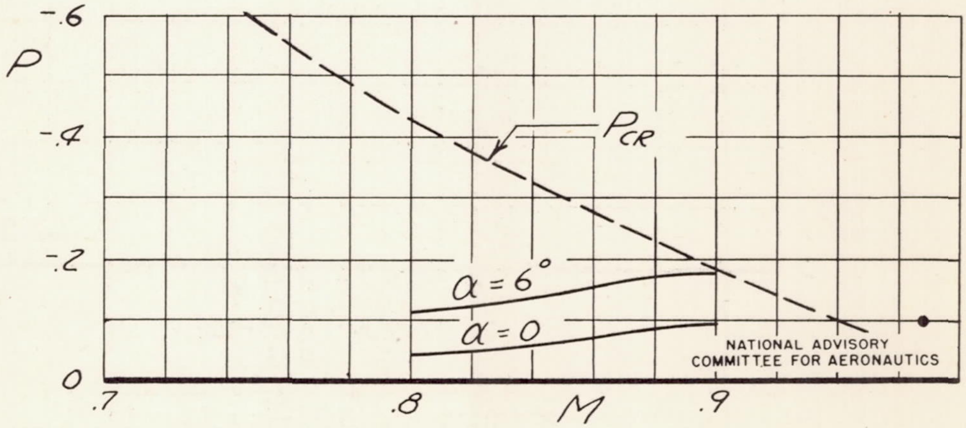

(b) MAXIMUM STATIC PRESSURE DECREASE ON THE TUNNEL WALL ABOVE THE WING ROOT OF THE MODEL

FIGURE 6.- PRESSURE MEASUREMENTS ABOUT THE MODEL SUPPORT SYSTEM WITH THE MODEL INSTALLED.

CONFIDENTIAL

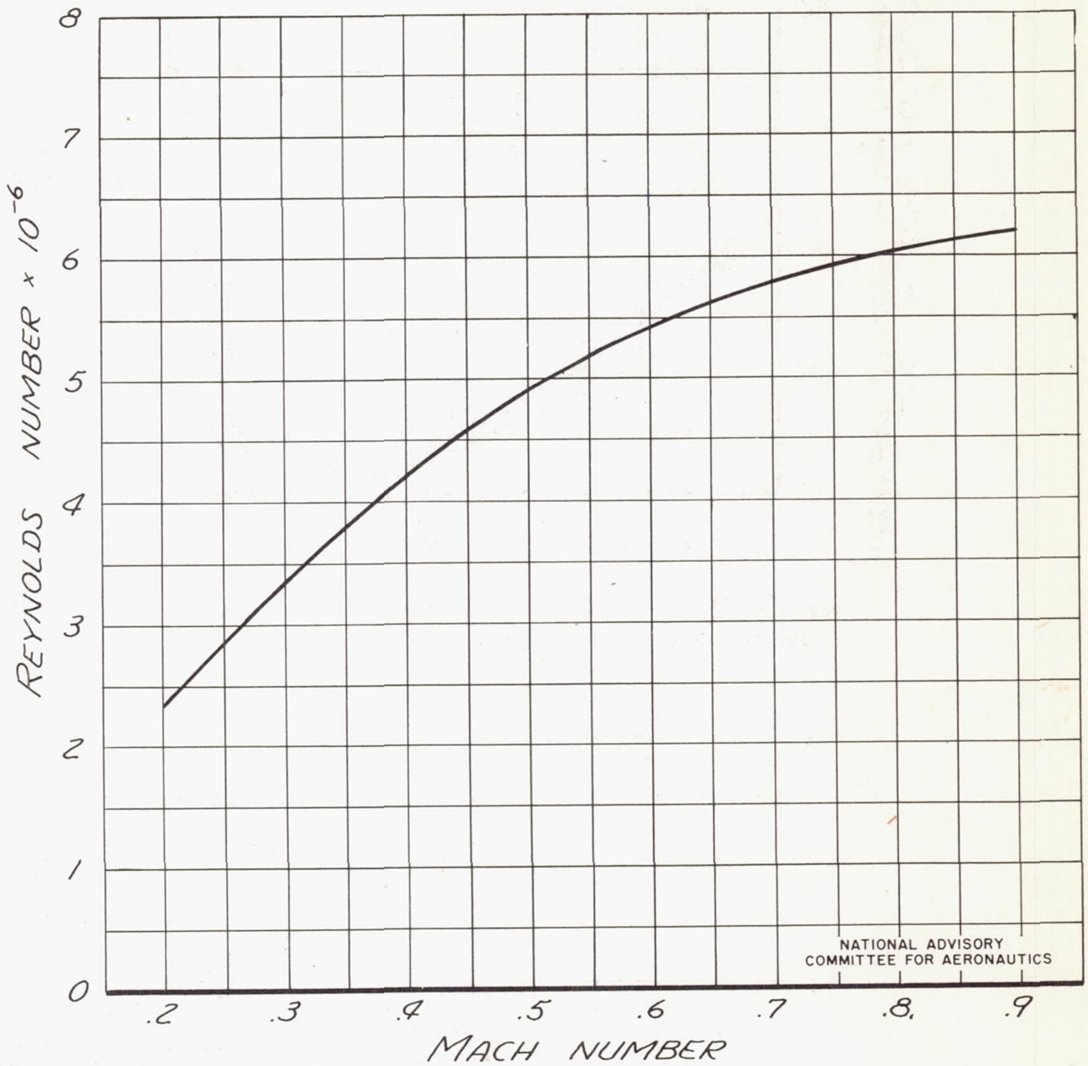

FIGURE 7.- VARIATION OF REYNOLDS NUMBER WITH MACH NUMBER FOR THE MODEL IN THE AMES 16-FOOT HIGH-SPEED WIND TUNNEL

CONFIDENTIAL

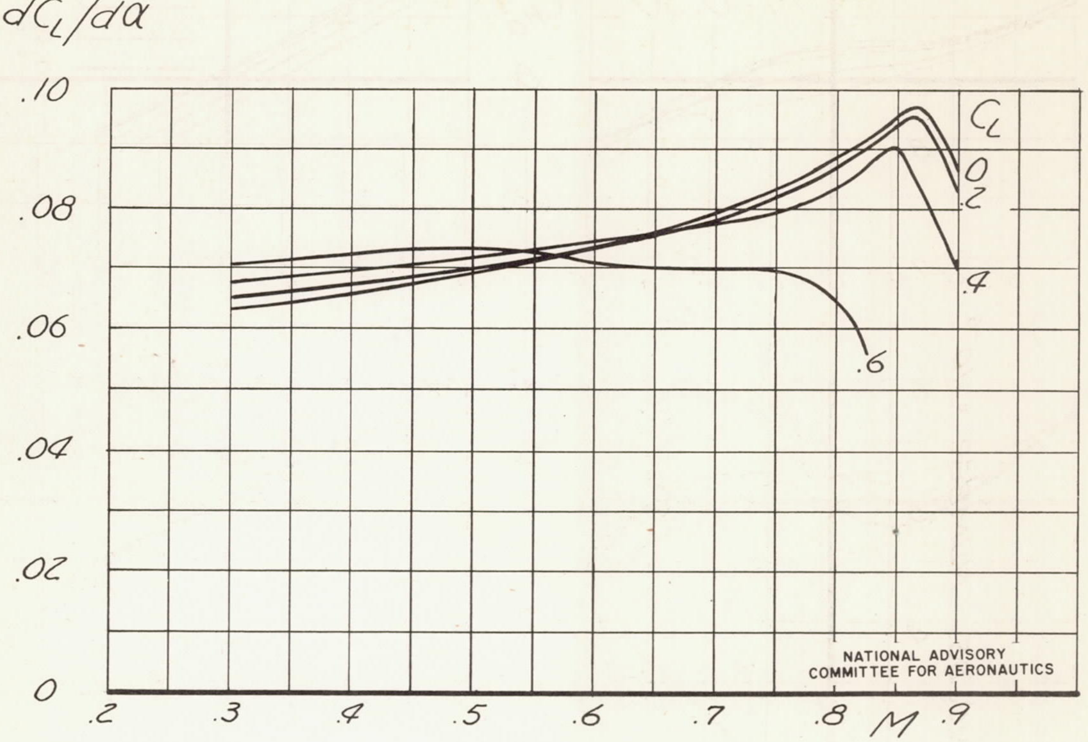

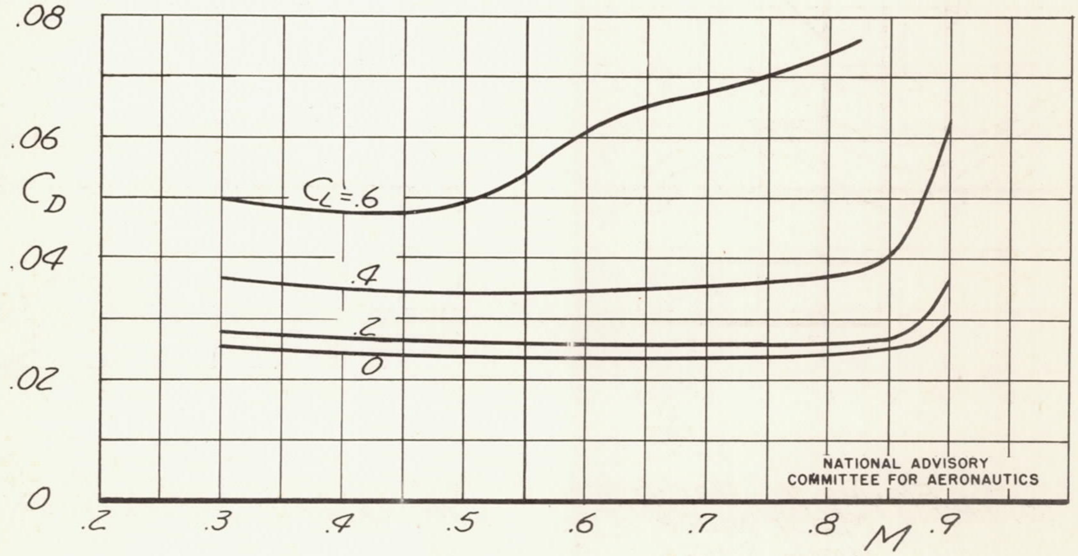

FIGURE 8.- LIFT AND DRAG CHARACTERISTICS FOR THE MODEL WITH THE TRUE-CONTOUR WING, TAIL OFF

CONFIDENTIAL

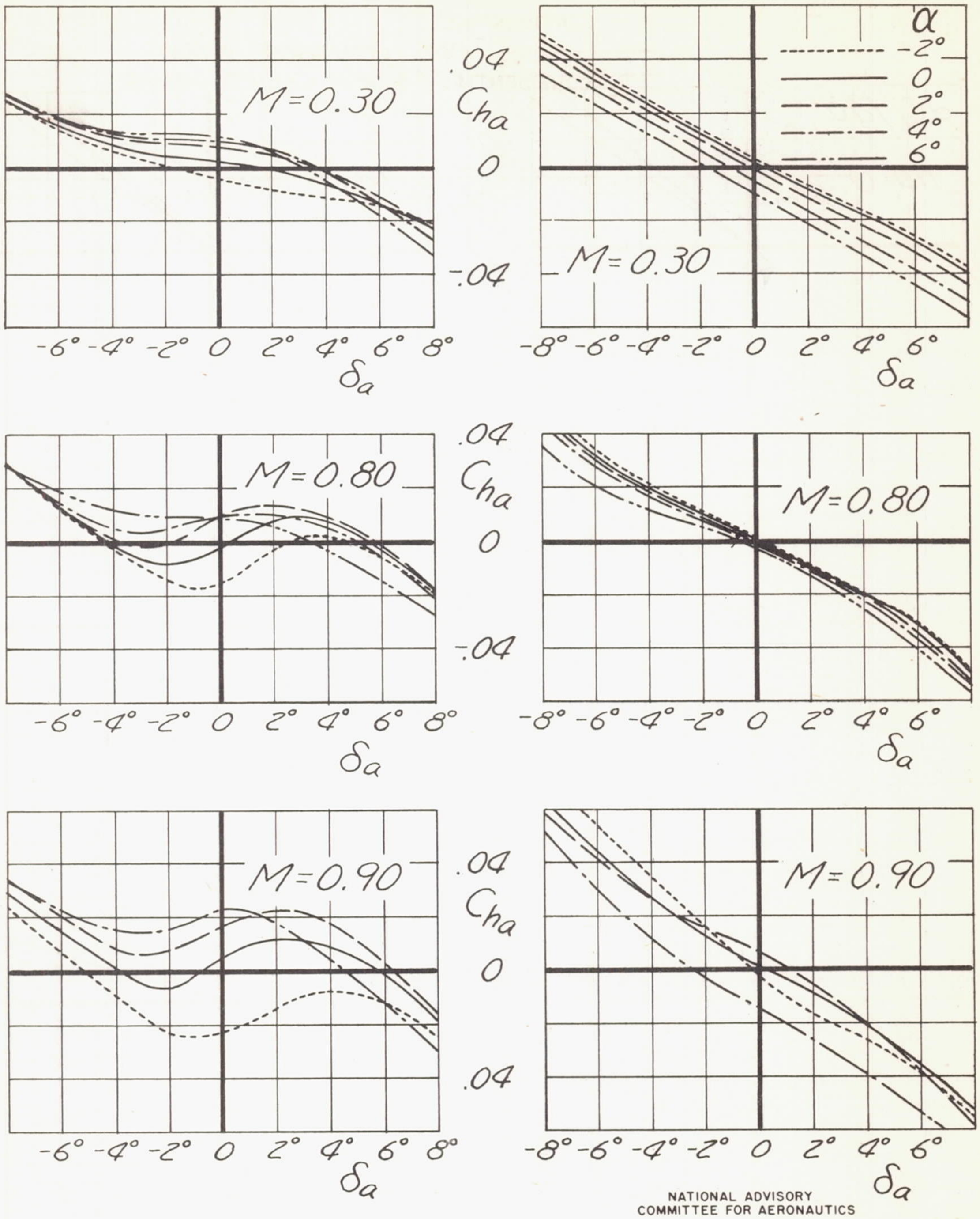

(a) TRUE-CONTOUR WING (b) EXTENDED-CHORD WING

FIGURE 9.- EFFECT OF WING TRAILING-EDGE CONTOUR ON THE AILERON HINGE MOMENT

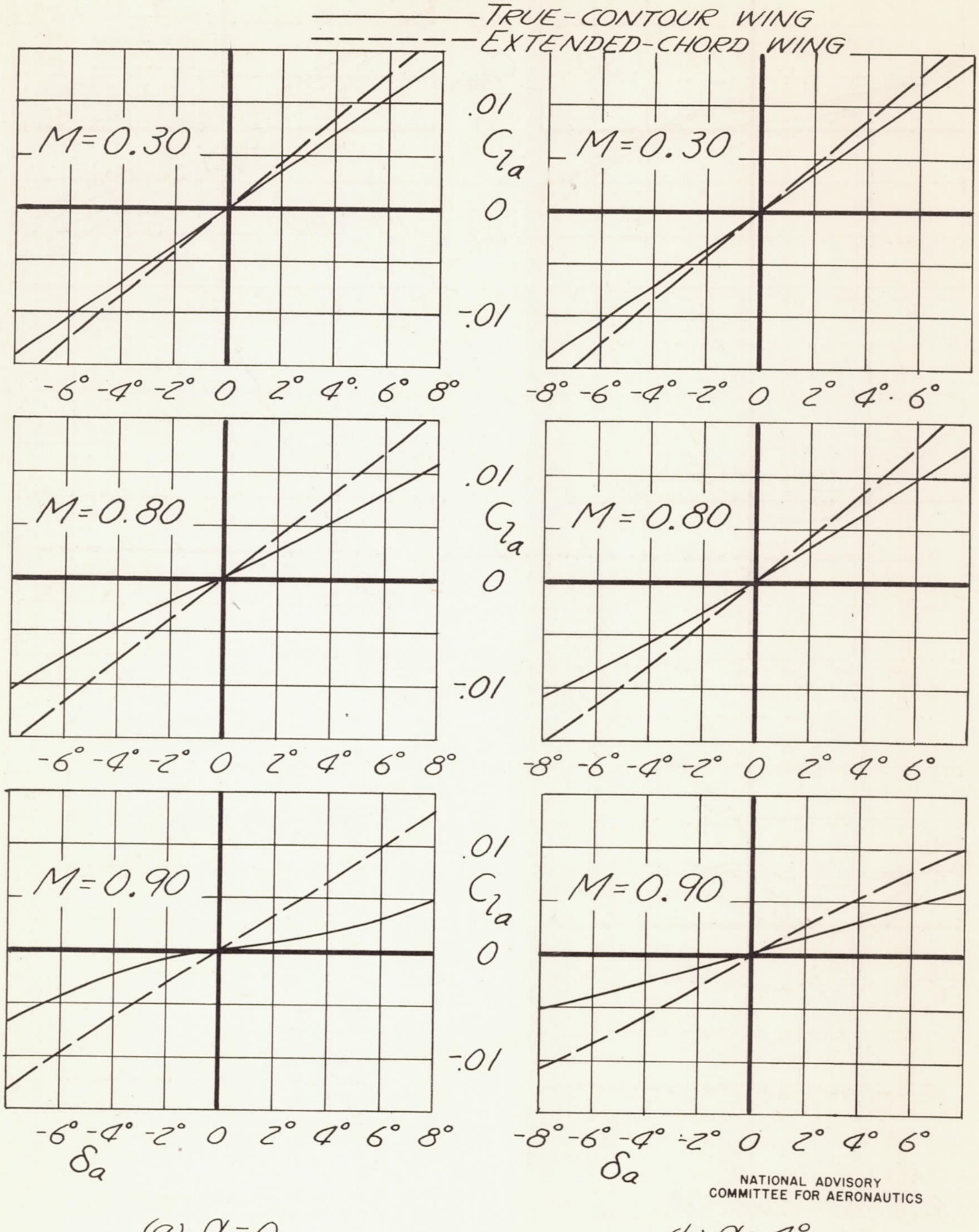

(a) $\alpha = 0$

(b) $\alpha = 4°$

FIGURE 10.- EFFECT OF WING TRAILING-EDGE CONTOUR ON AILERON EFFECTIVENESS

CONFIDENTIAL

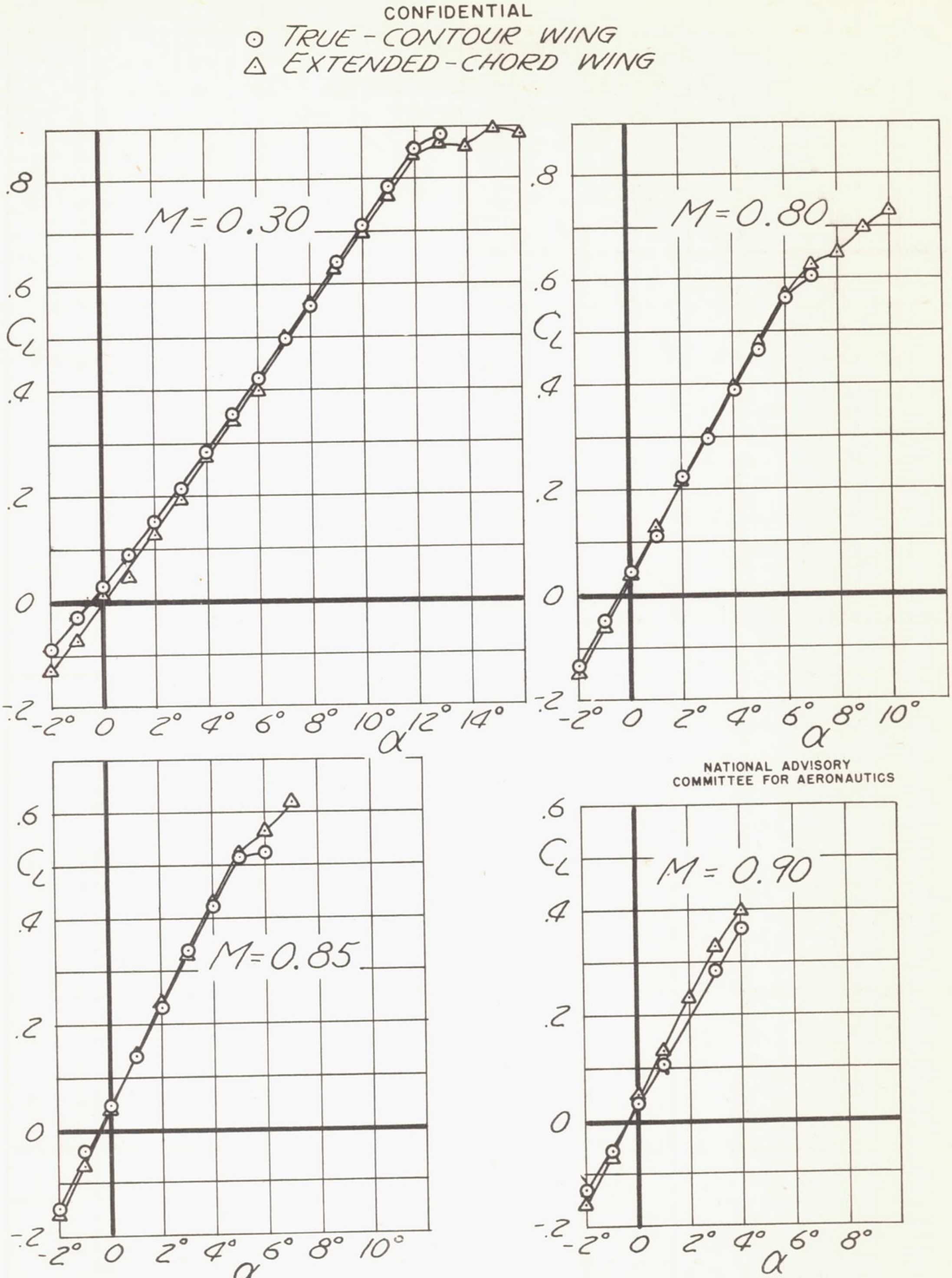

FIGURE 11.-EFFECT OF WING TRAILING-EDGE CONTOUR ON THE TAIL-OFF LIFT

CONFIDENTIAL

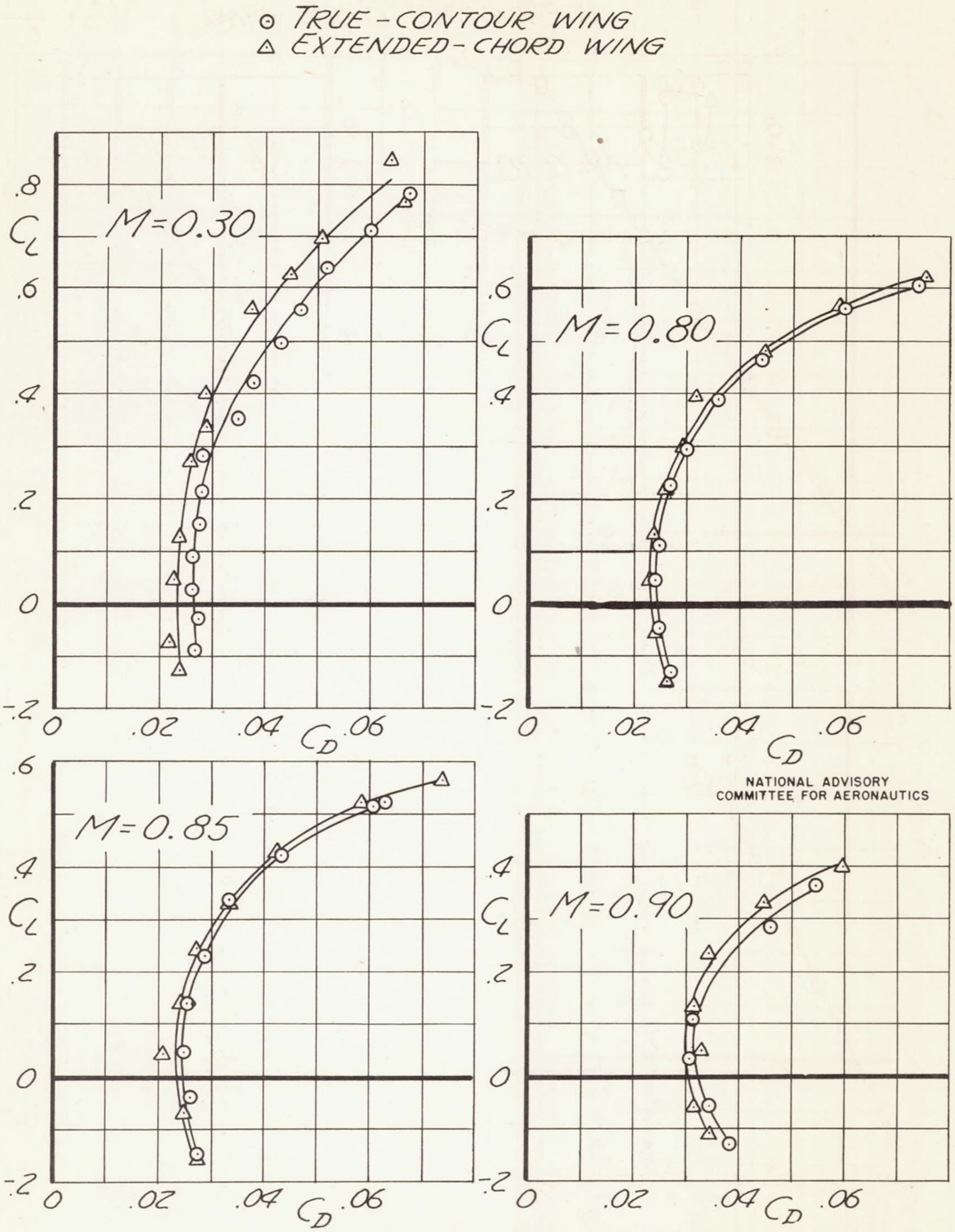

FIGURE 12.-EFFECT OF WING TRAILING-EDGE CONTOUR ON THE TAIL-OFF DRAG

CONFIDENTIAL

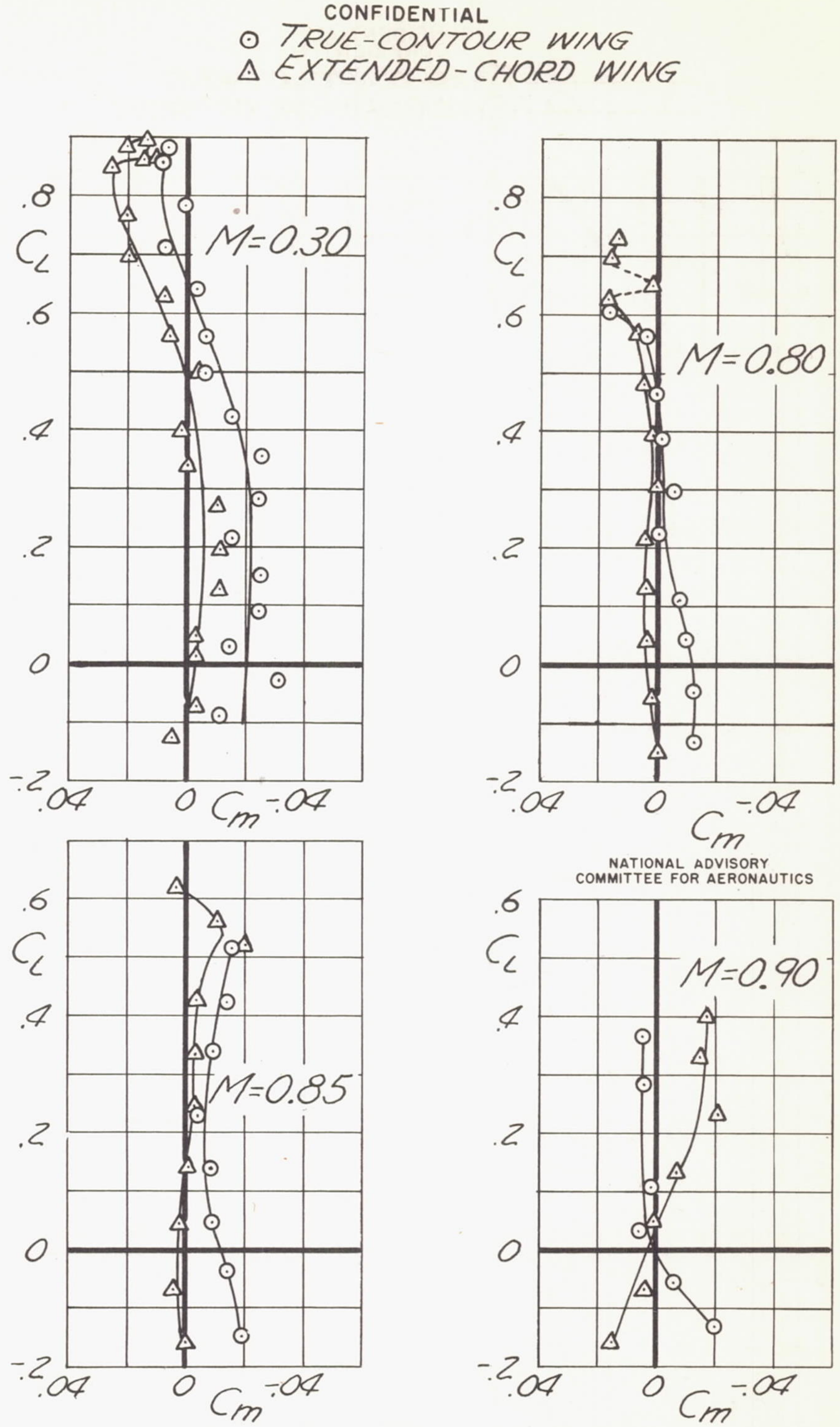

FIGURE 13.– EFFECT OF WING TRAILING-EDGE CONTOUR ON THE TAIL-OFF PITCHING MOMENT

CONFIDENTIAL

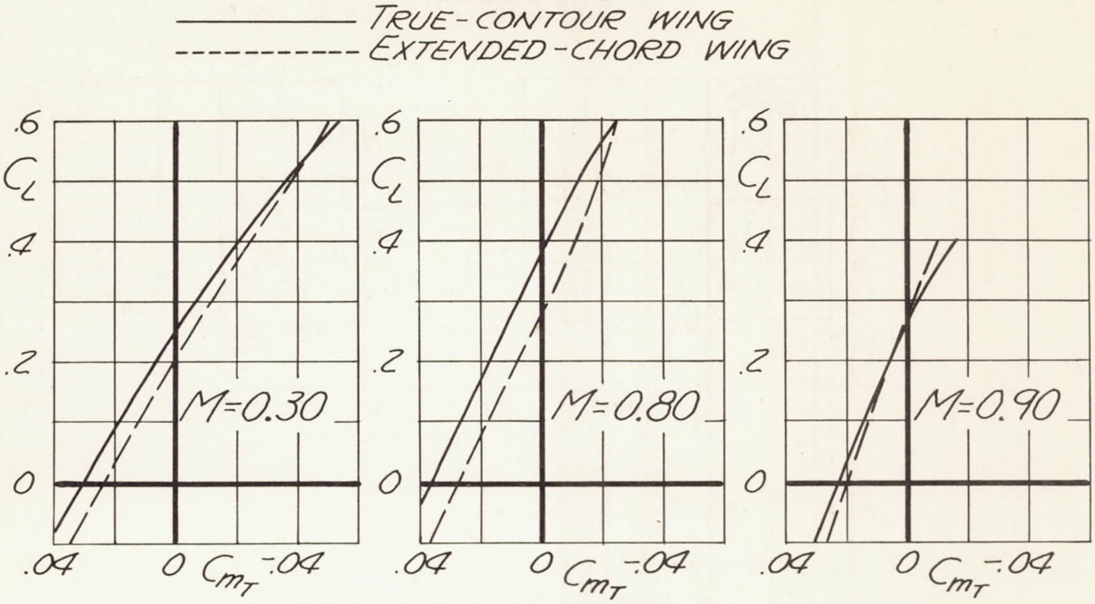

(a) PITCHING-MOMENT COEFFICIENT DUE TO HORIZONTAL TAIL

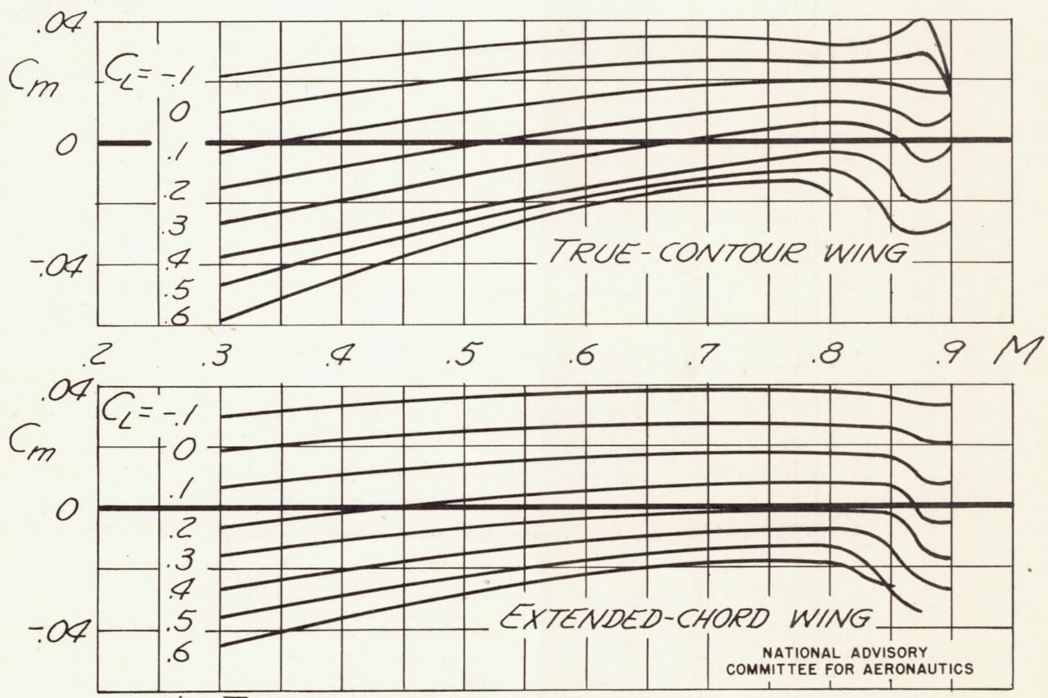

(b) TAIL-ON PITCHING MOMENT

FIGURE 14.– EFFECT OF WING TRAILING-EDGE CONTOUR ON THE TAIL-ON PITCHING MOMENT

CONFIDENTIAL

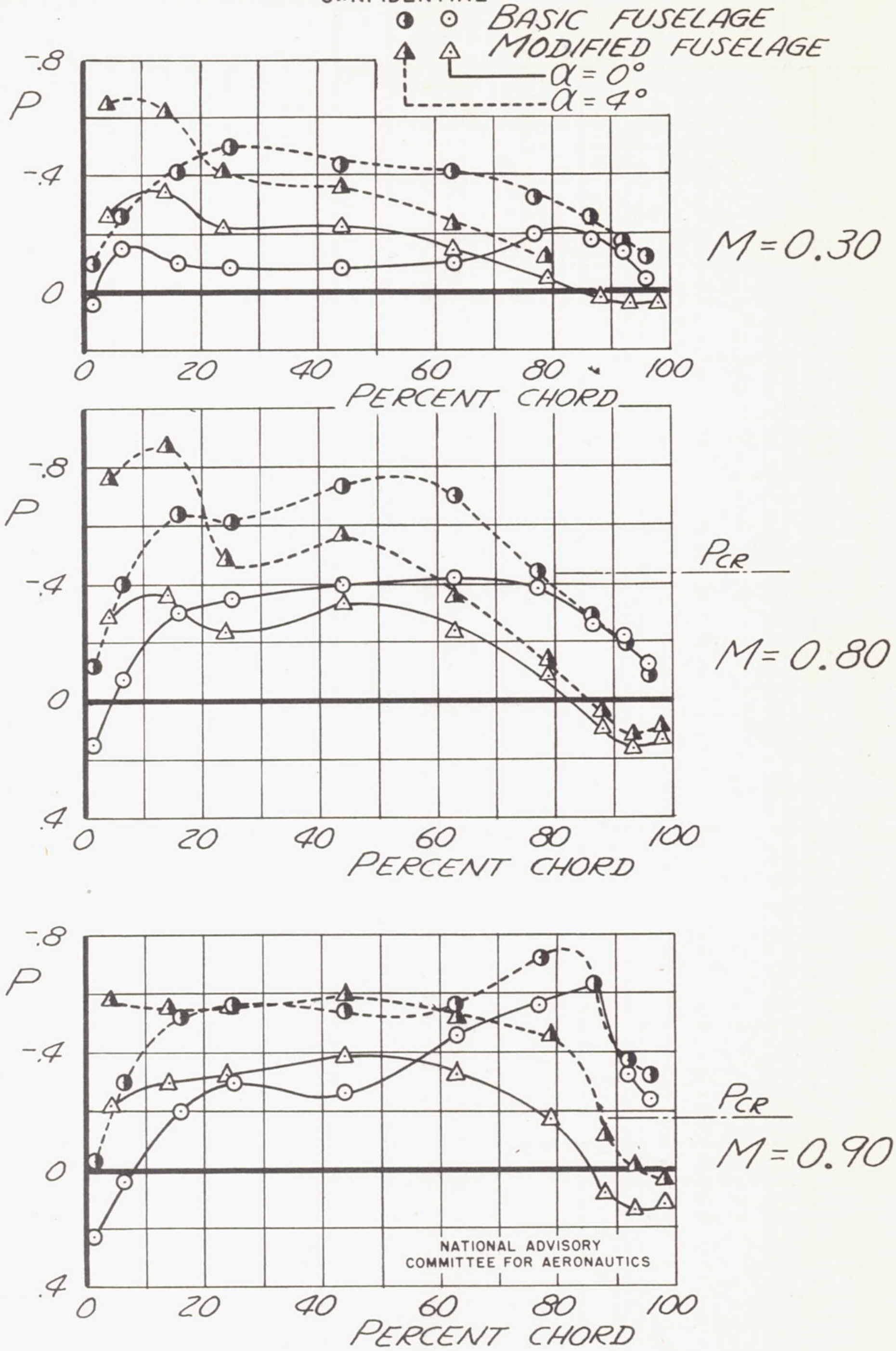

FIGURE 15.– EFFECT OF FUSELAGE CONTOUR ON THE PRESSURE DISTRIBUTION ALONG THE WING-FUSELAGE INTERSECTION.

CONFIDENTIAL

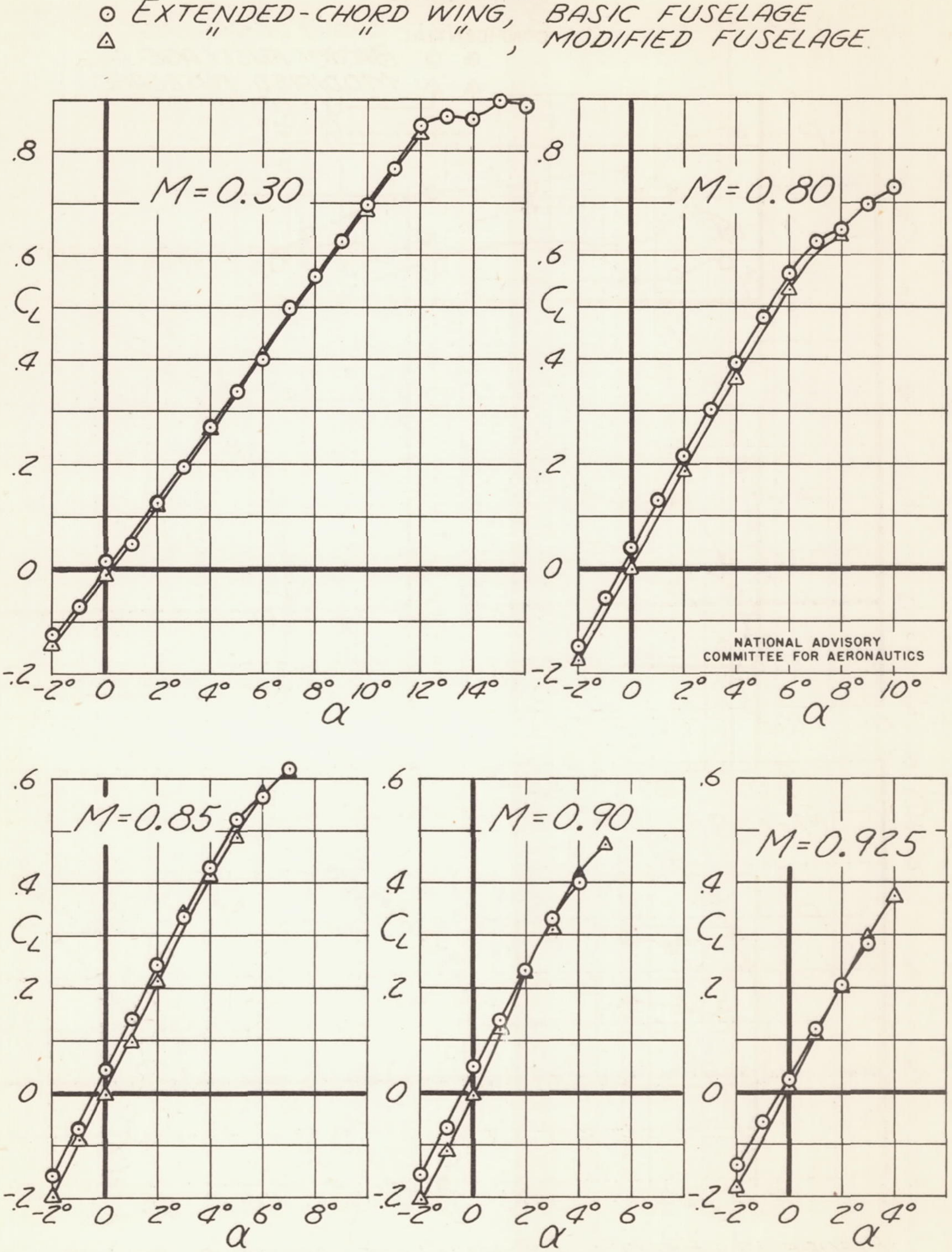

FIGURE 16.– EFFECT OF FUSELAGE CONTOUR ON THE TAIL-OFF LIFT

CONFIDENTIAL

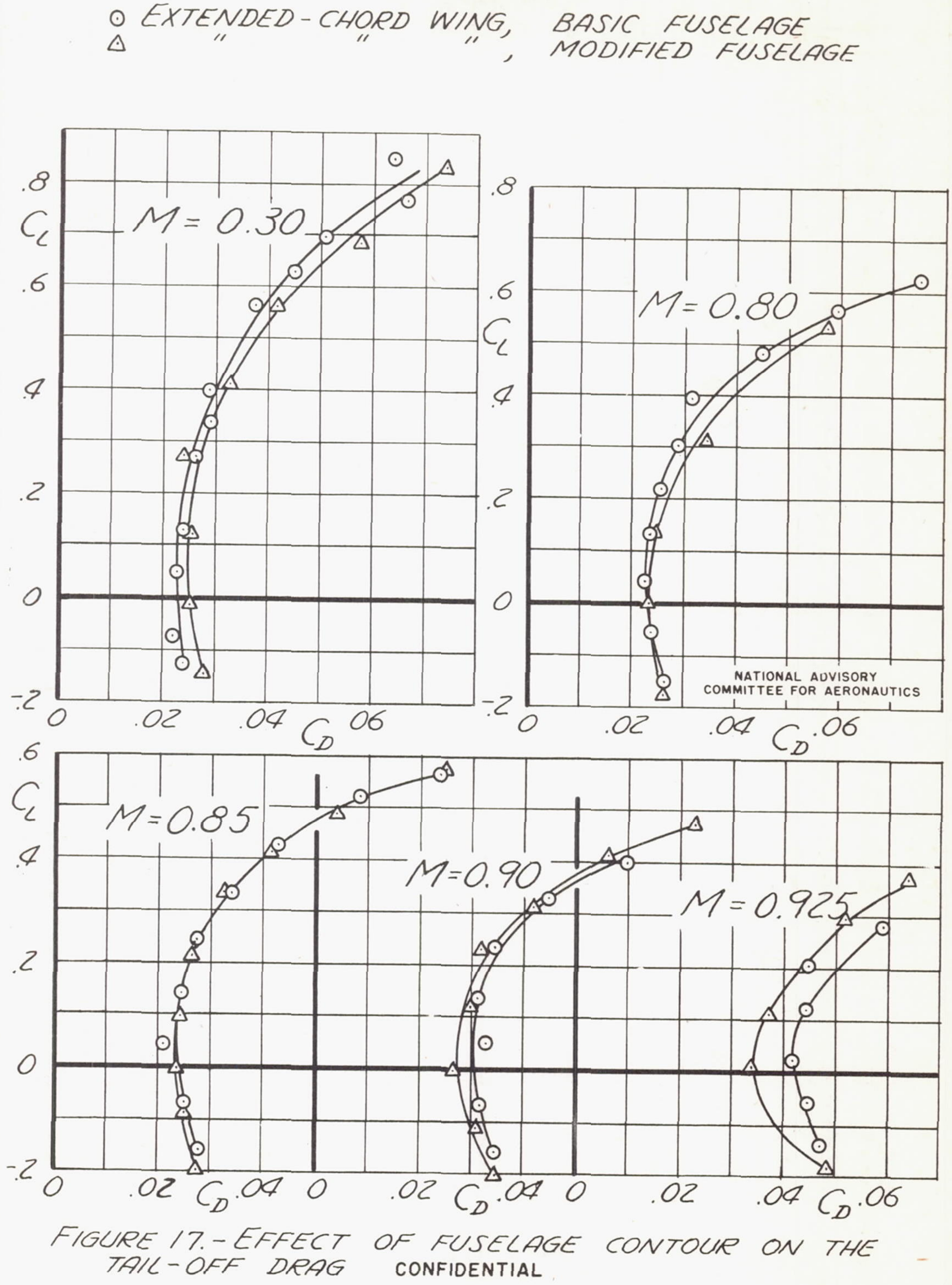

FIGURE 17.- EFFECT OF FUSELAGE CONTOUR ON THE TAIL-OFF DRAG

CONFIDENTIAL

CONFIDENTIAL

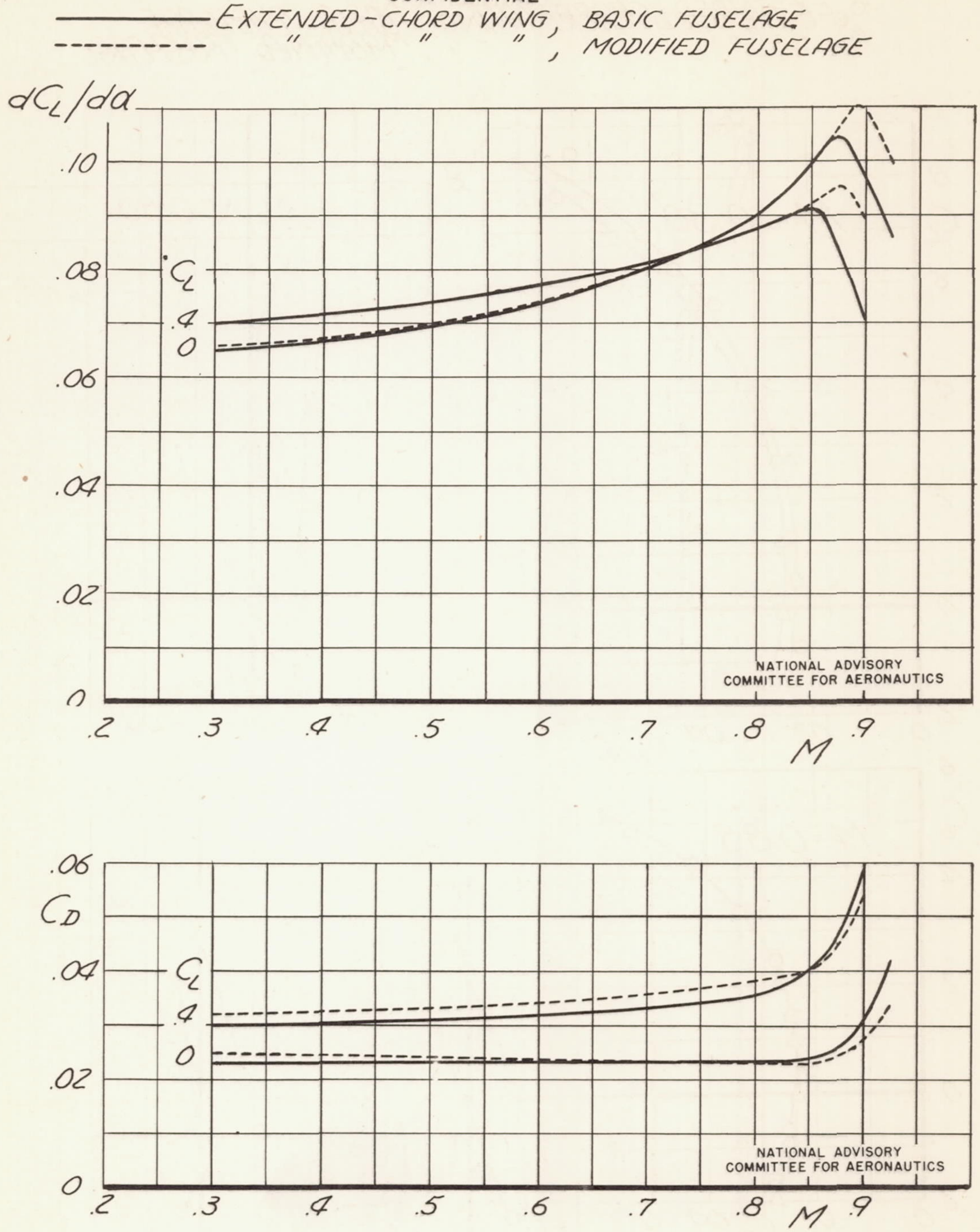

FIGURE 18. - EFFECT OF FUSELAGE CONTOUR ON THE VARIATION OF LIFT-CURVE SLOPE AND DRAG COEFFICIENT WITH MACH NUMBER

CONFIDENTIAL

CONFIDENTIAL

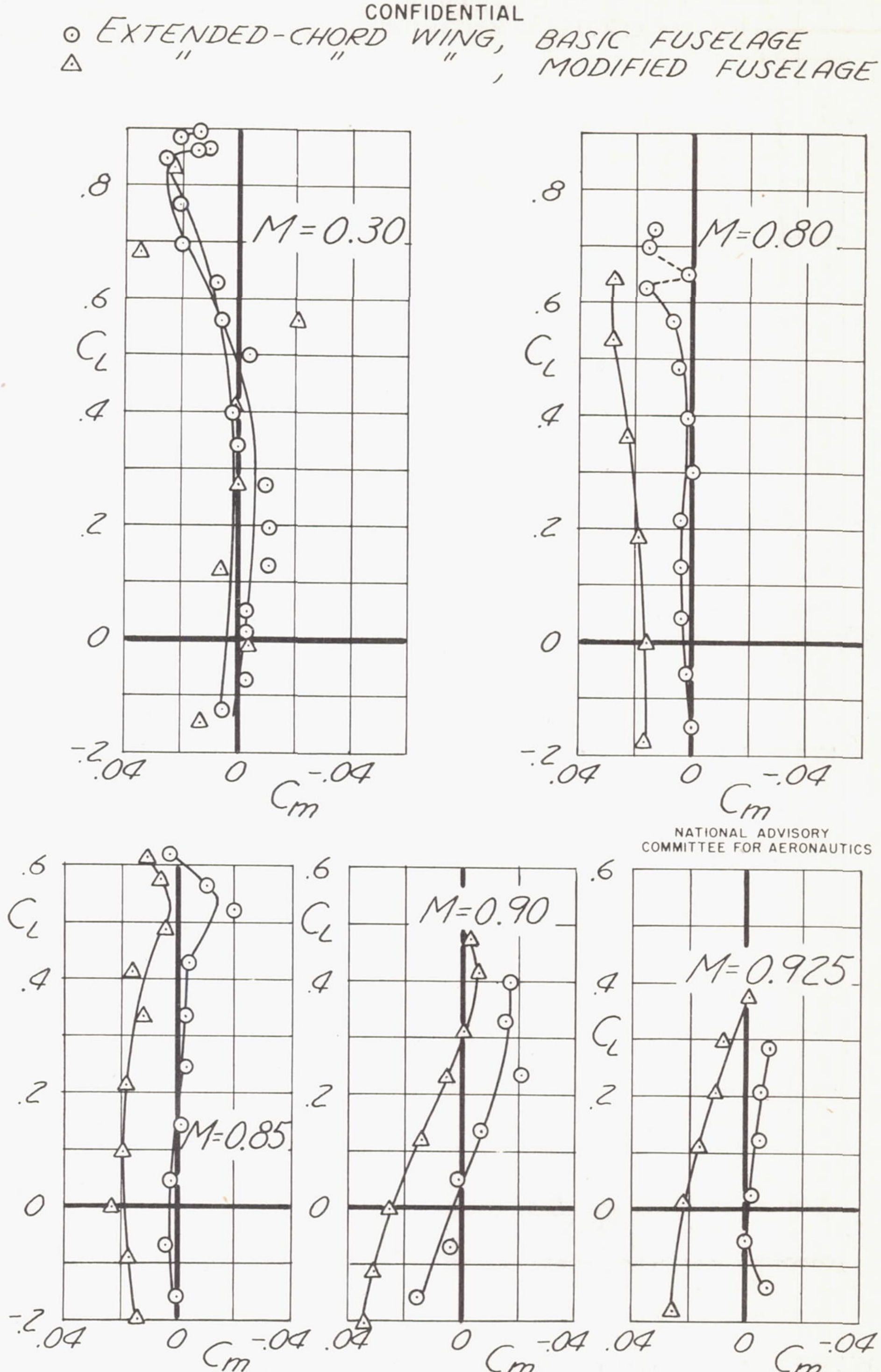

FIGURE 19.- EFFECT OF FUSELAGE CONTOUR ON THE TAIL-OFF PITCHING MOMENT

CONFIDENTIAL

CONFIDENTIAL

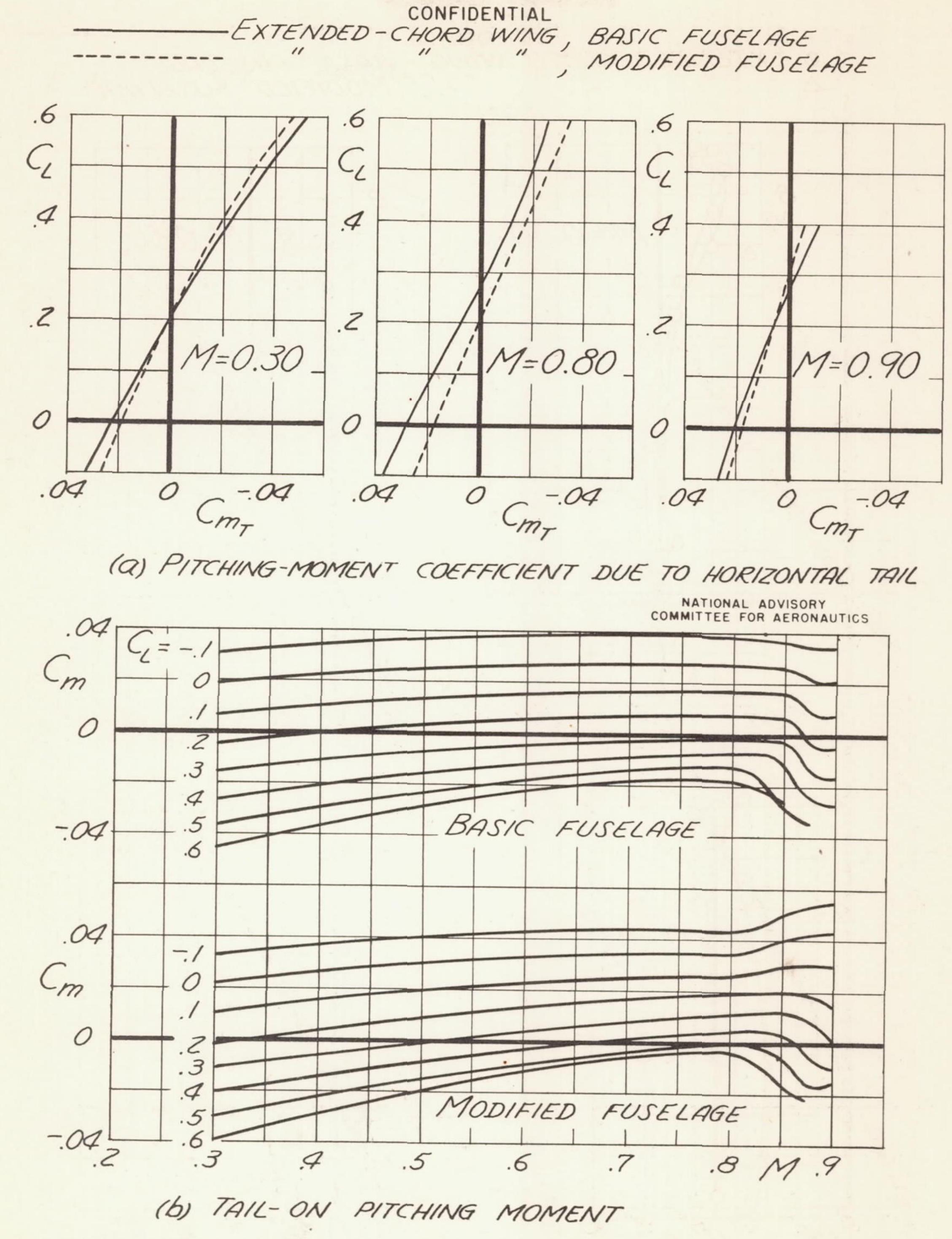

FIGURE 20.- EFFECT OF FUSELAGE CONTOUR ON THE TAIL-ON PITCHING MOMENT

CONFIDENTIAL

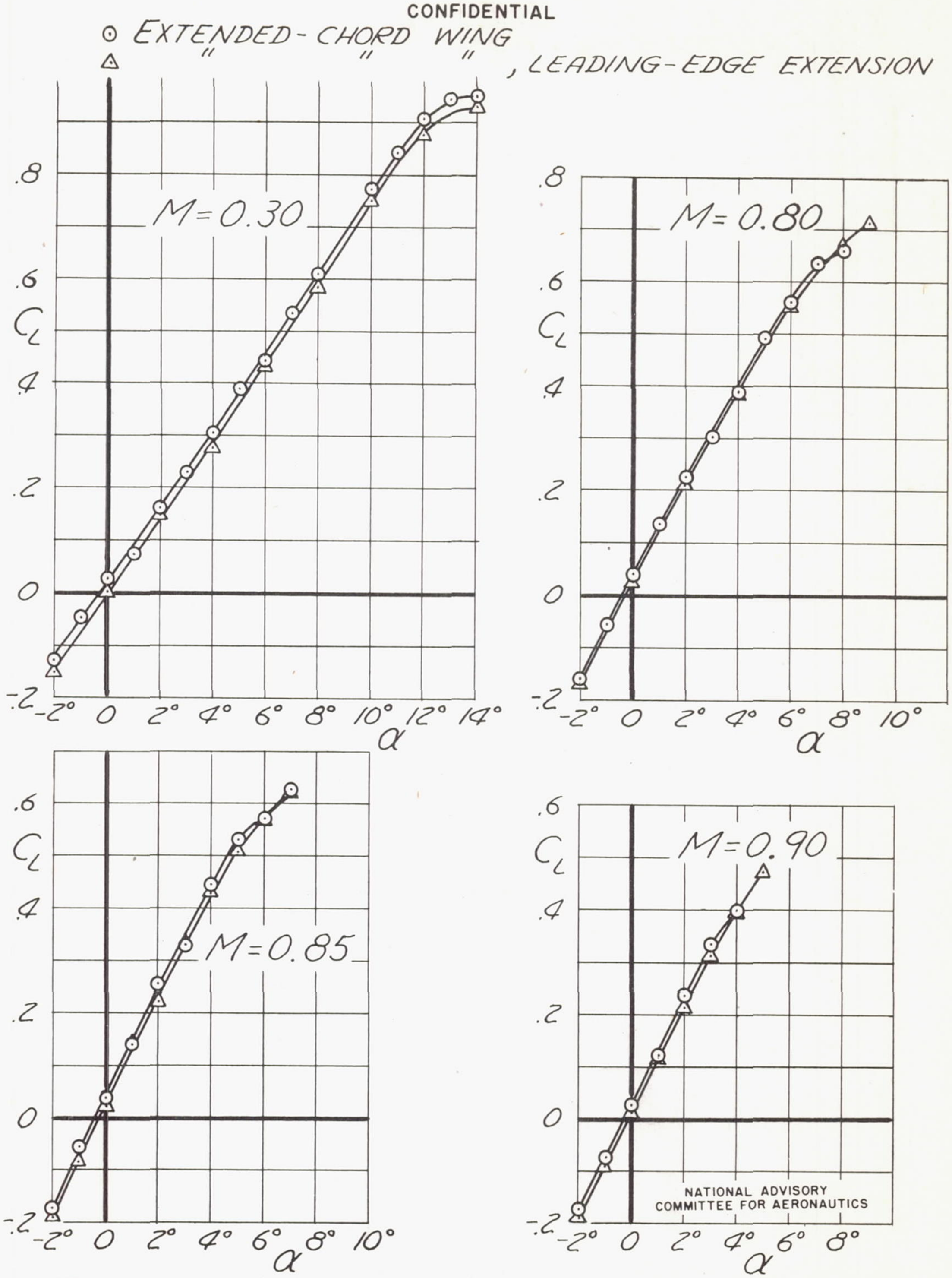

FIGURE 21.– EFFECT OF WING LEADING-EDGE EXTENSION ON THE TAIL-ON LIFT

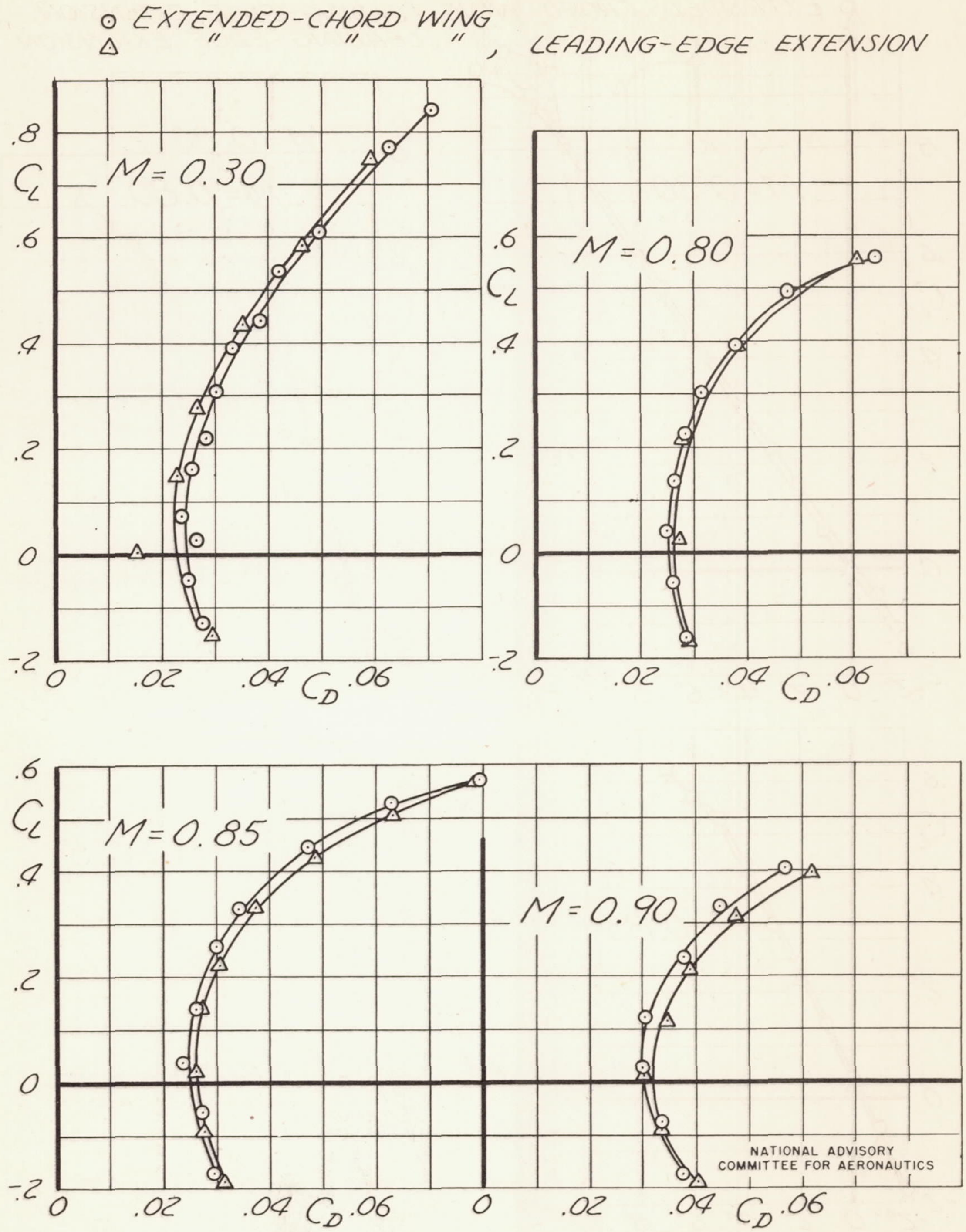

FIGURE 22.- EFFECT OF WING LEADING-EDGE EXTENSION ON THE TAIL-ON DRAG

CONFIDENTIAL

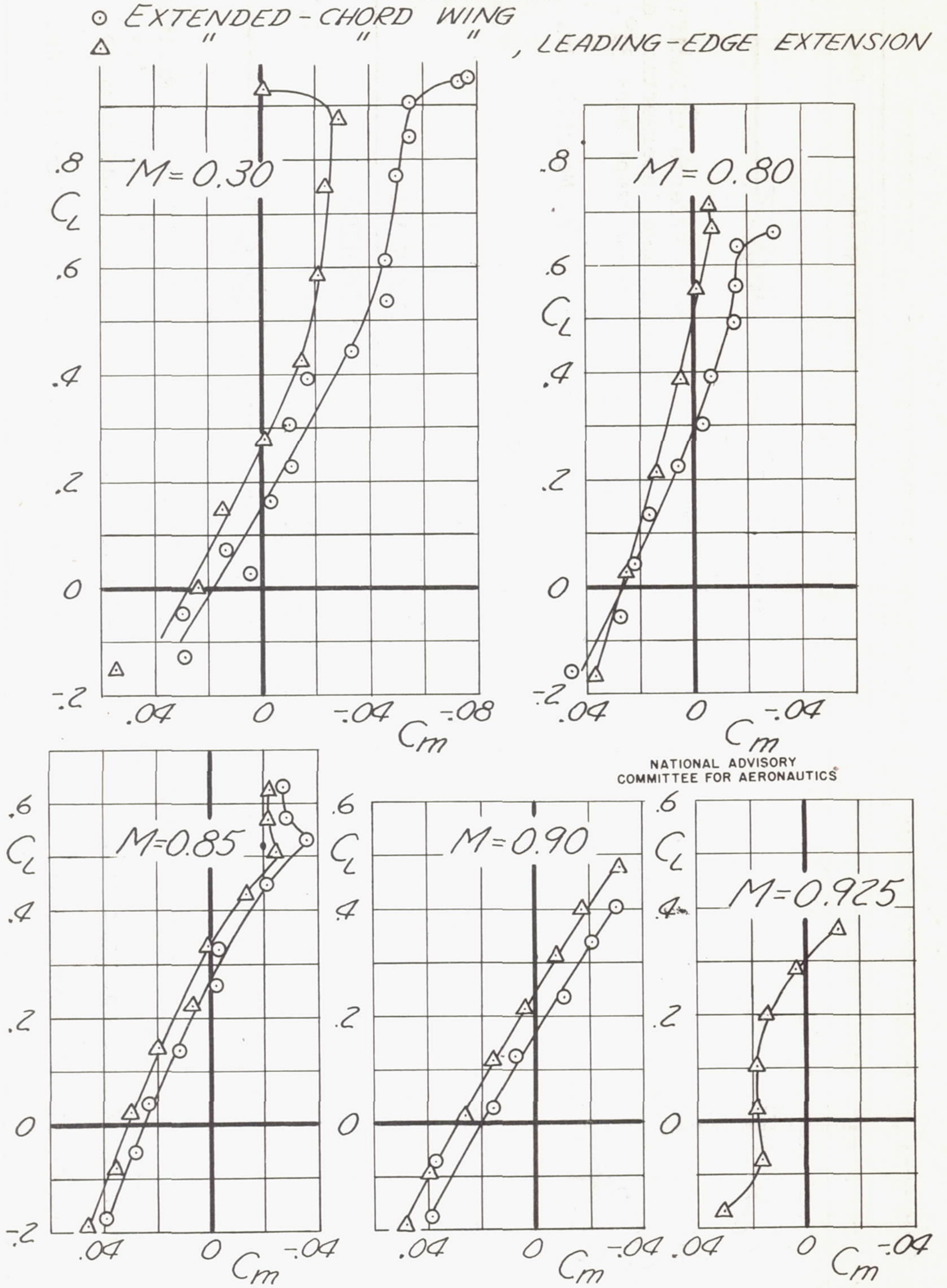

FIGURE 23.-EFFECT OF WING LEADING-EDGE EXTENSION ON THE TAIL-ON PITCHING MOMENT

CONFIDENTIAL